What makes a wall/filament?

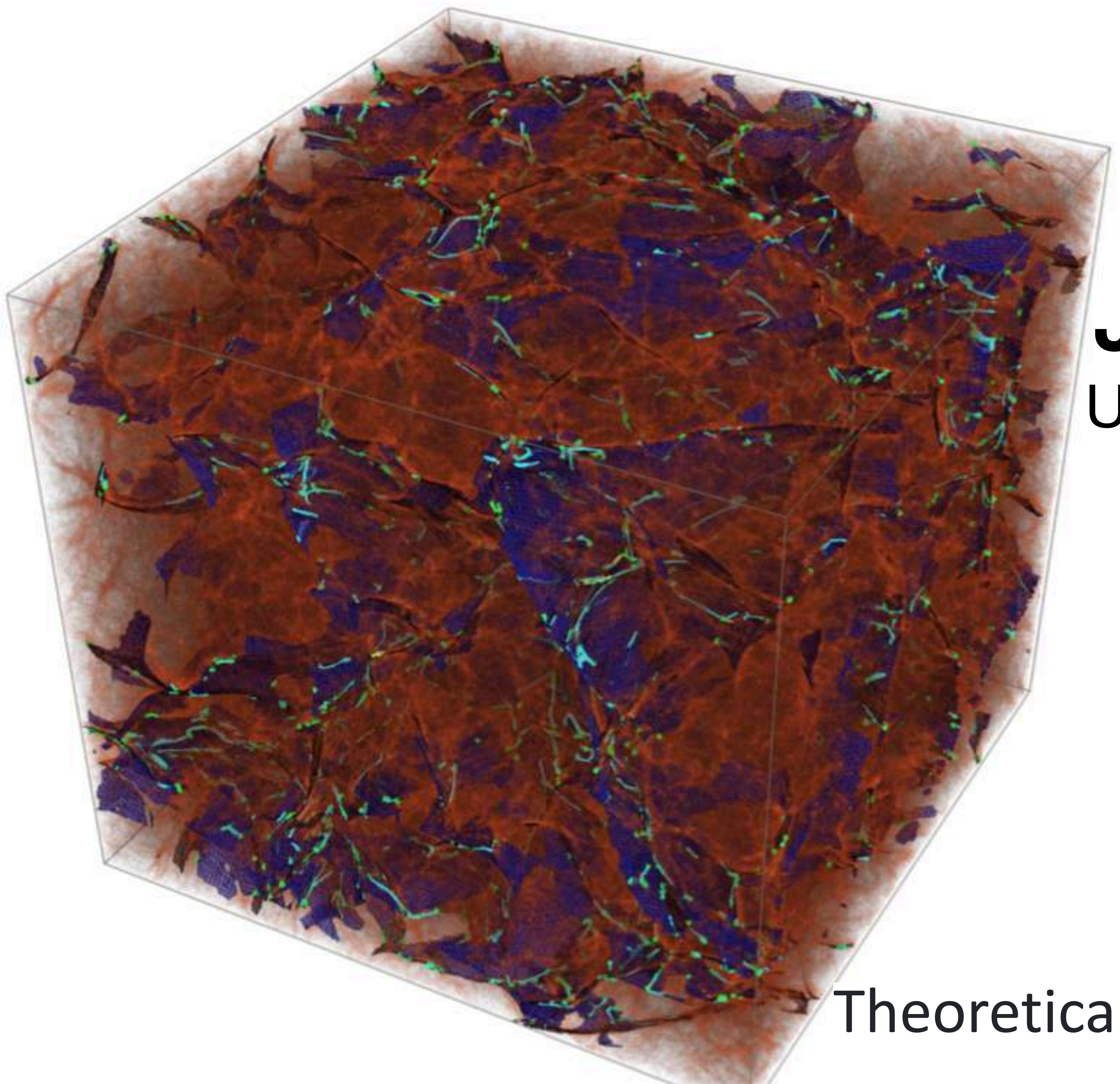

Job Feldbrugge
University of Edinburgh

Work in collaboration with
Rien van de Weygaert,
Benjamin Hertzsch,
Maé Rodriguez

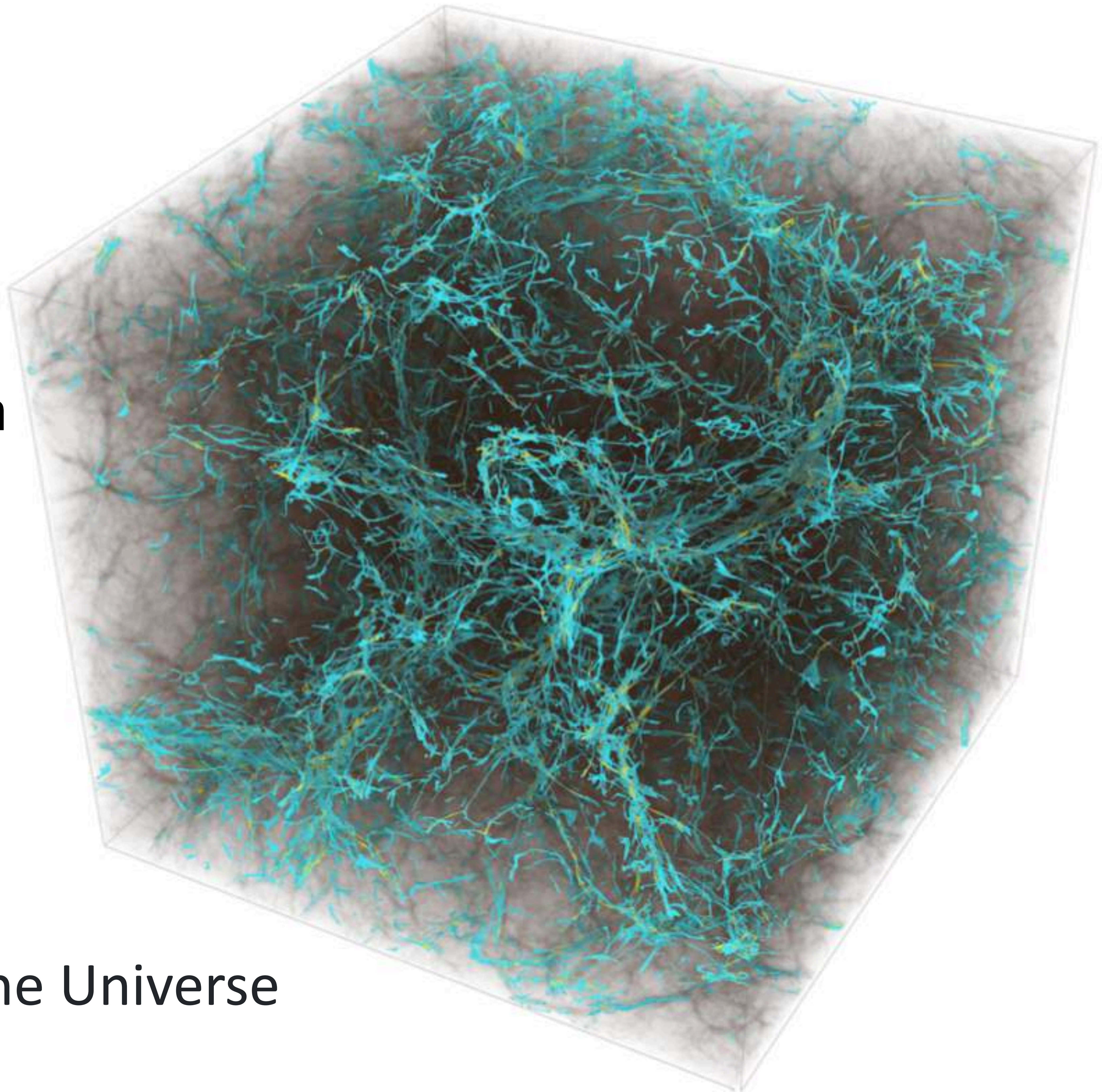

3rd of June 2024

Theoretical Modeling of LSS of the Universe

The cosmic web

The simple initial fluctuations are close to Gaussian.

This collapses into an intricate cosmic web with **voids**, **walls**, **filaments**, and **clusters**, inheriting this information

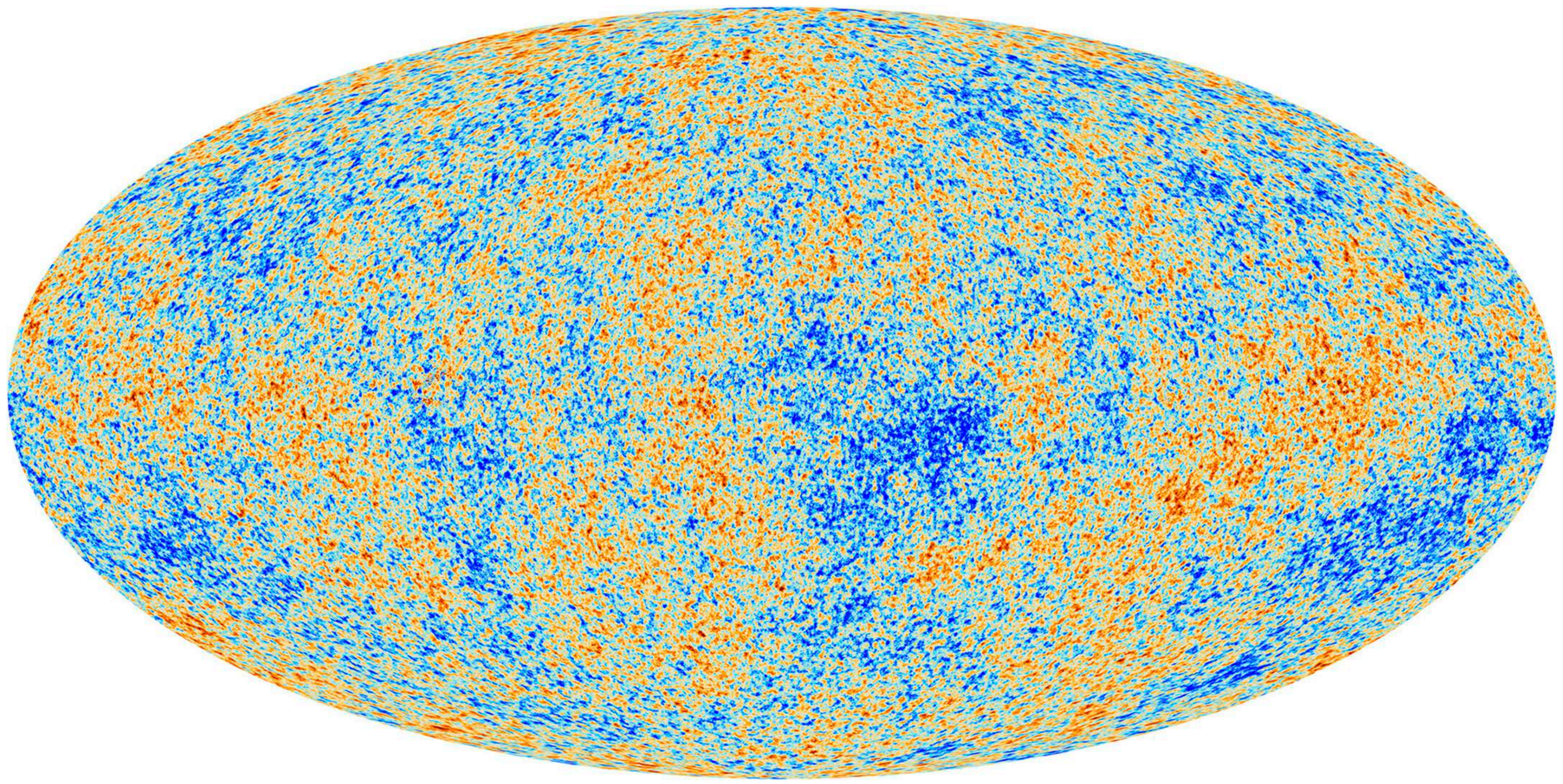

Planck Satellite

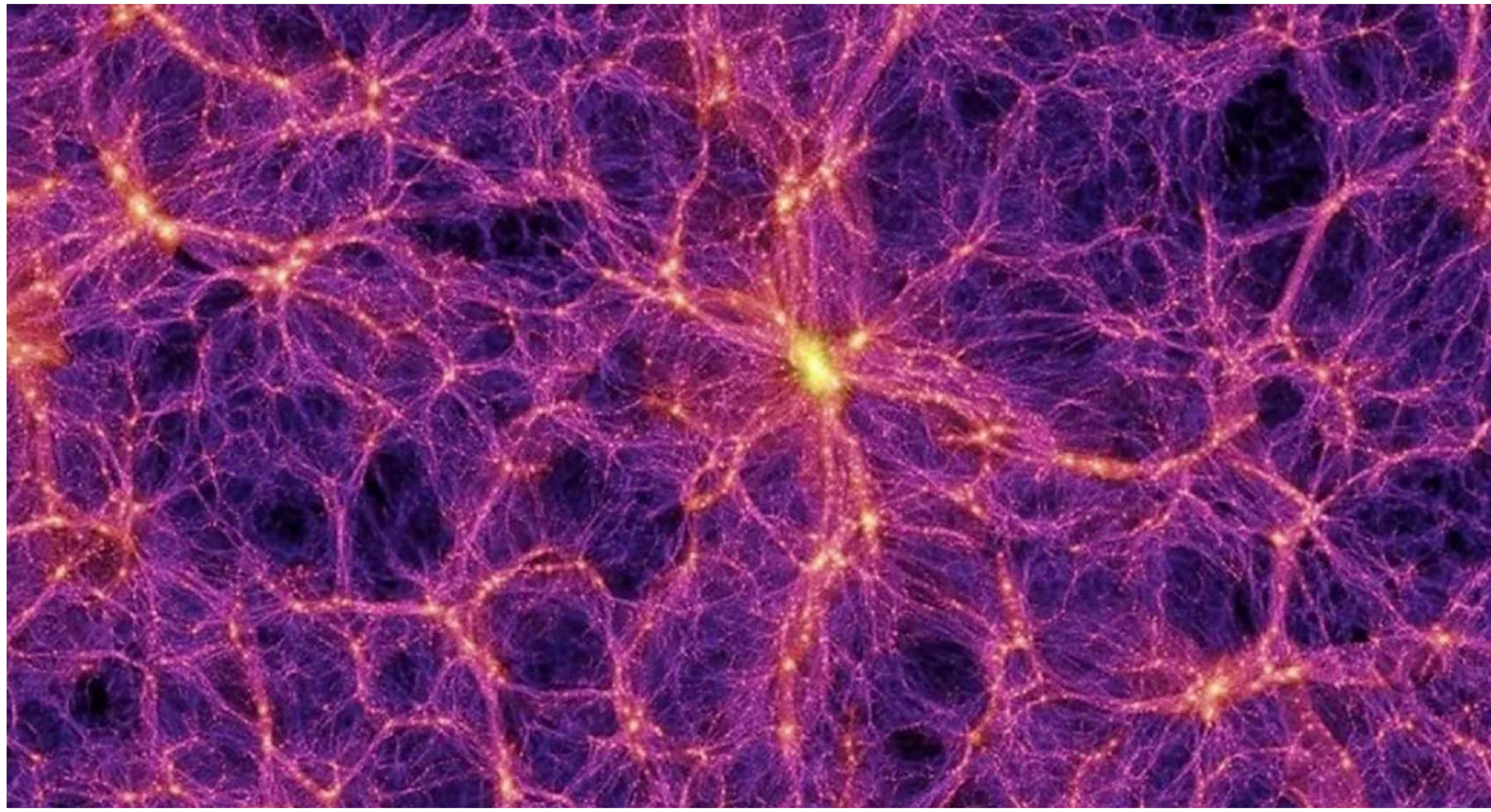

Millenium simulation

The cosmic web

The simple initial fluctuations are close to Gaussian.

This collapses into an intricate cosmic web with **voids**, **walls**, **filaments**, and **clusters**, inheriting this information

What makes a patch in Lagrangian space from into a wall or filament?

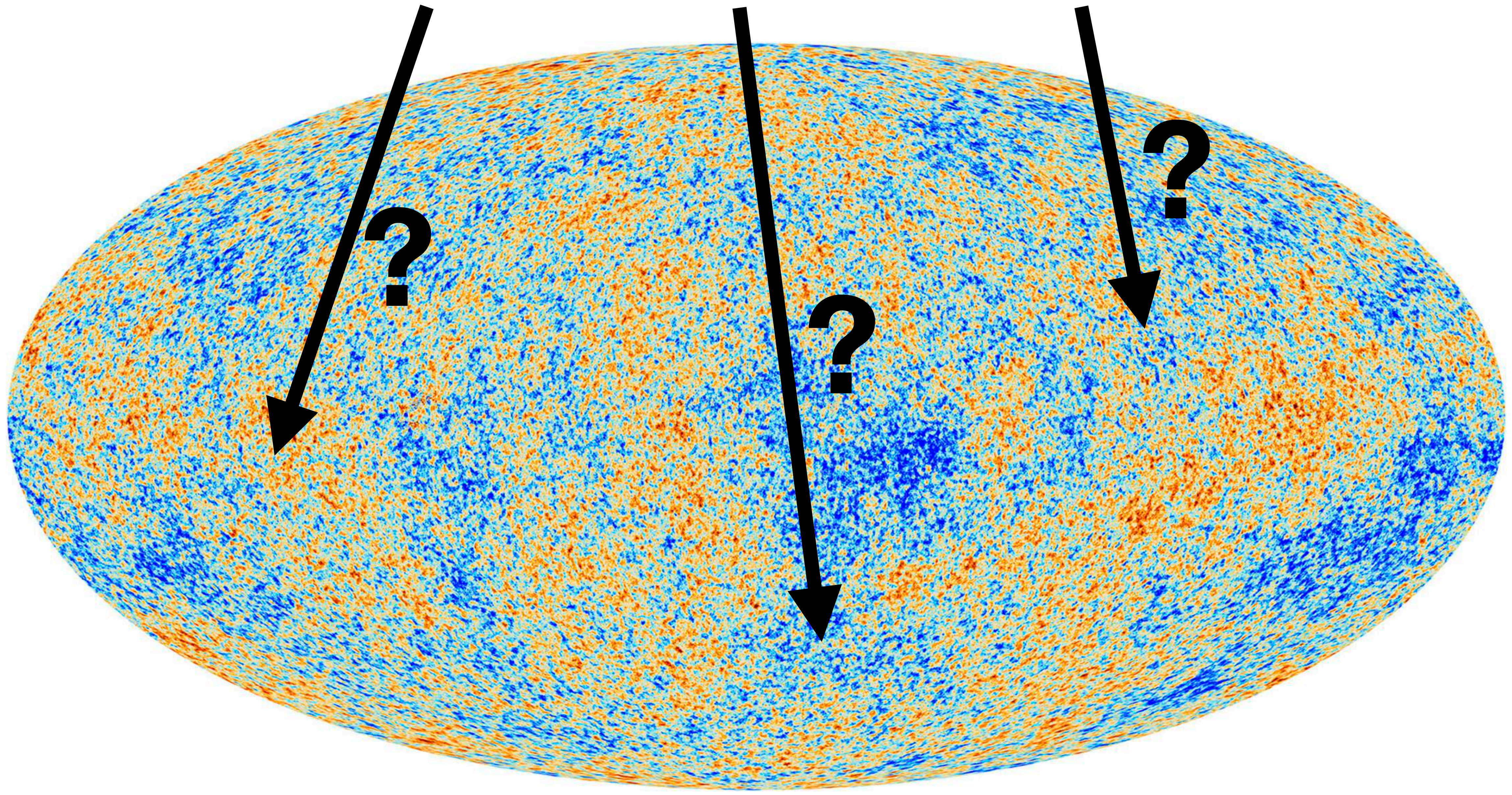

Planck Satellite

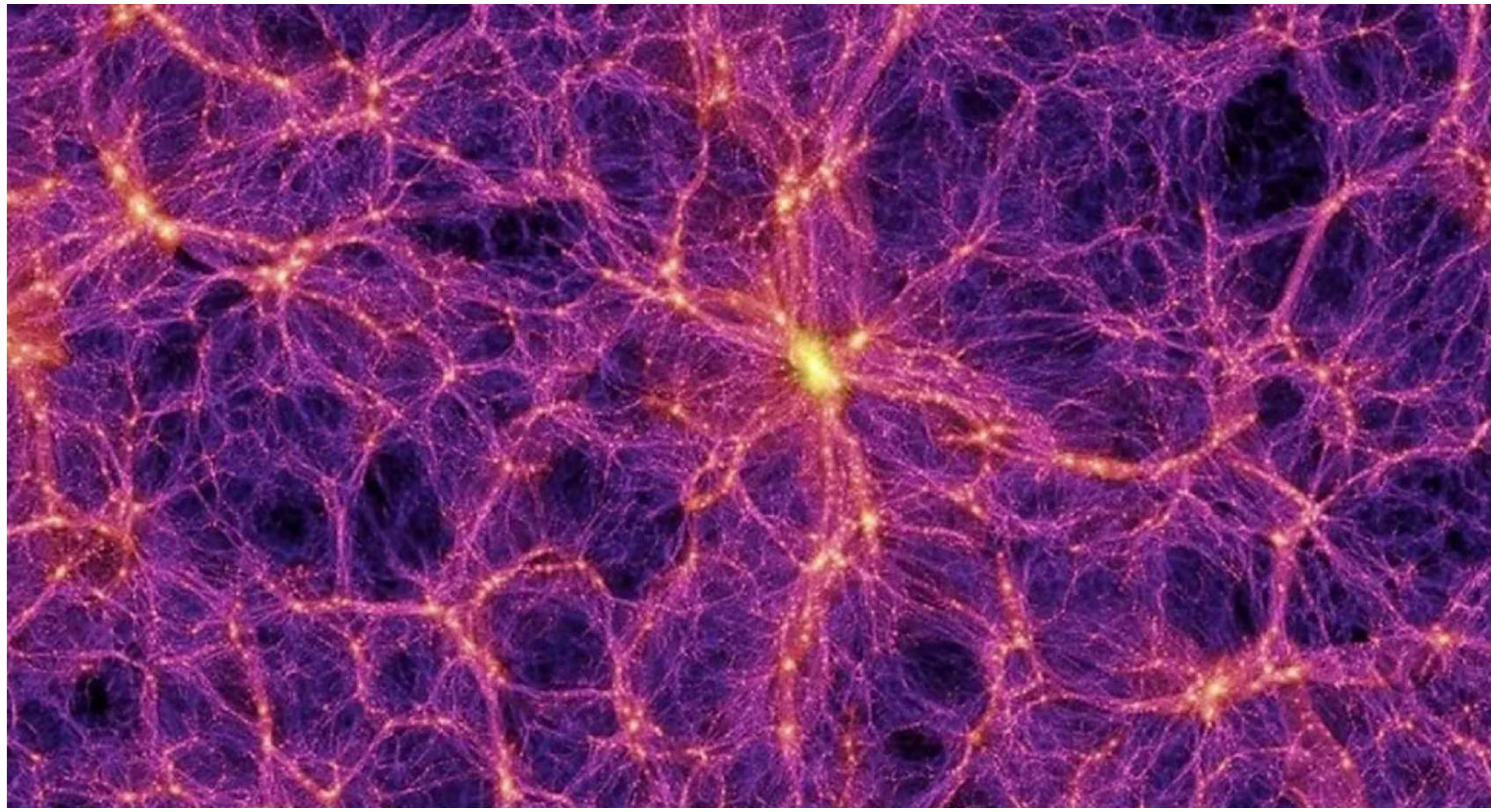

Millenium simulation

Caustics

In **non-linear gravitational collapse** the geometric structure follows the geometry of the **multi-stream regions**

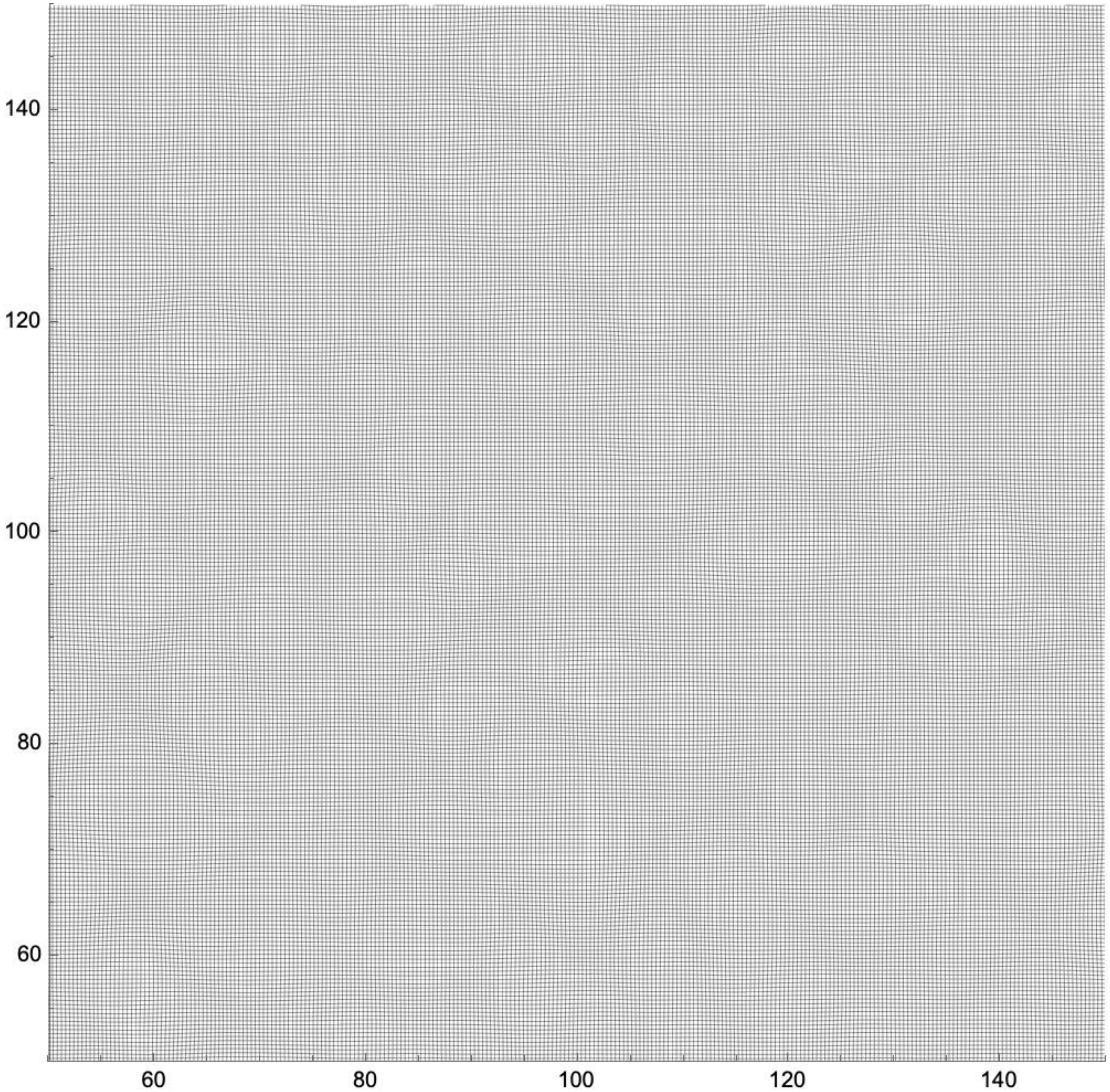

Caustics

- Dark matter forms the geometric structure of the cosmic web through formation of multi-stream regions

- The caustics bound the multi-stream regions

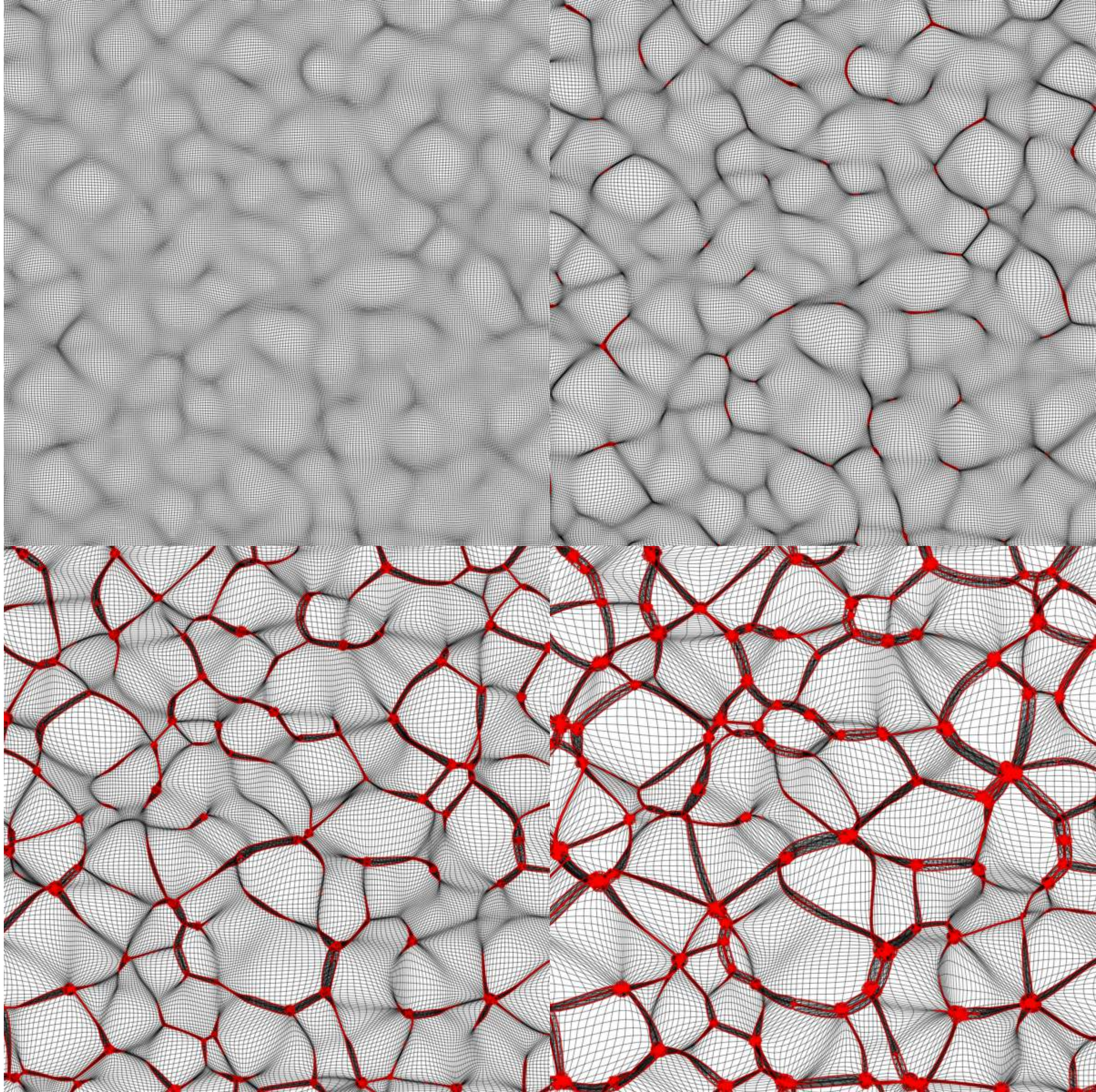

Caustics

- *Vladimir Arnol'd* extended *René Thom's* classification of stable degenerate critical points to **Lagrangian catastrophe theory**
- The **classification of caustics** was applied to *large-scale structure formation* to predict the geometric structure of the *cosmic web*

1972 NORMAL FORMS FOR FUNCTIONS NEAR DEGENERATE CRITICAL POINTS, THE WEYL GROUPS OF A_k, D_k, E_k AND LAGRANGIAN SINGULARITIES

V. I. Arnol'd

1980 EVOLUTION OF SINGULARITIES OF POTENTIAL FLOWS IN COLLISION-FREE MEDIA AND THE METAMORPHOSIS OF CAUSTICS IN THREE-DIMENSIONAL SPACE

V. I. Arnol'd

1982 The Large Scale Structure of the Universe I. General Properties. One- and Two-Dimensional Models

V. I. ARNOLD
Moscow State University, U.S.S.R.

and

S. F. SHANDARIN and YA. B. ZELDOVICH
Institute of Applied Mathematics, Moscow, U.S.S.R.

(*Received August* 11, 1981)

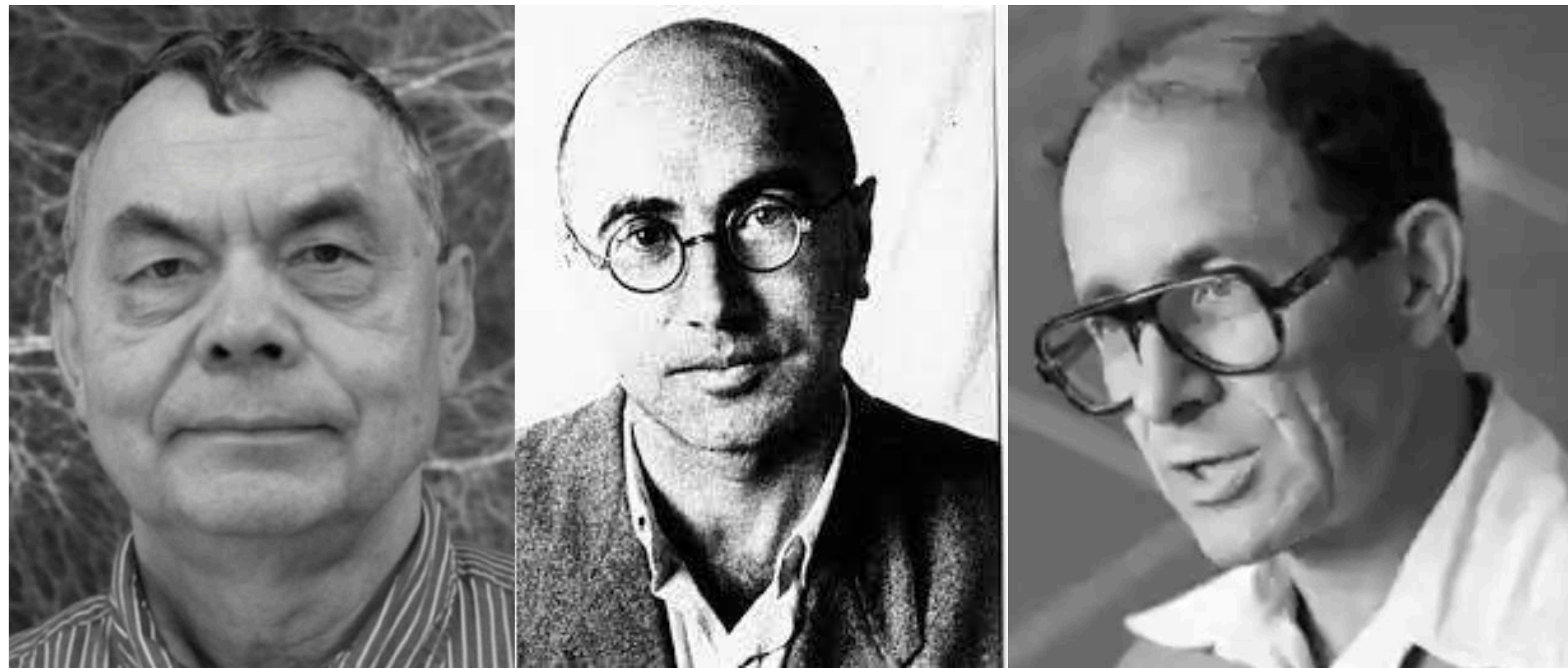

Caustics

Arnol'd, Shandarin, Zel'dovich (1982)

Lagrangian fluid dynamics

$$\mathbf{x}_t(\mathbf{q}) = \mathbf{q} + \mathbf{s}_t(\mathbf{q})$$

where the displacement map solves the Euler equation and the Poisson equation while implementing the conservation of mass. The density follows as the reciprocal of the Jacobian

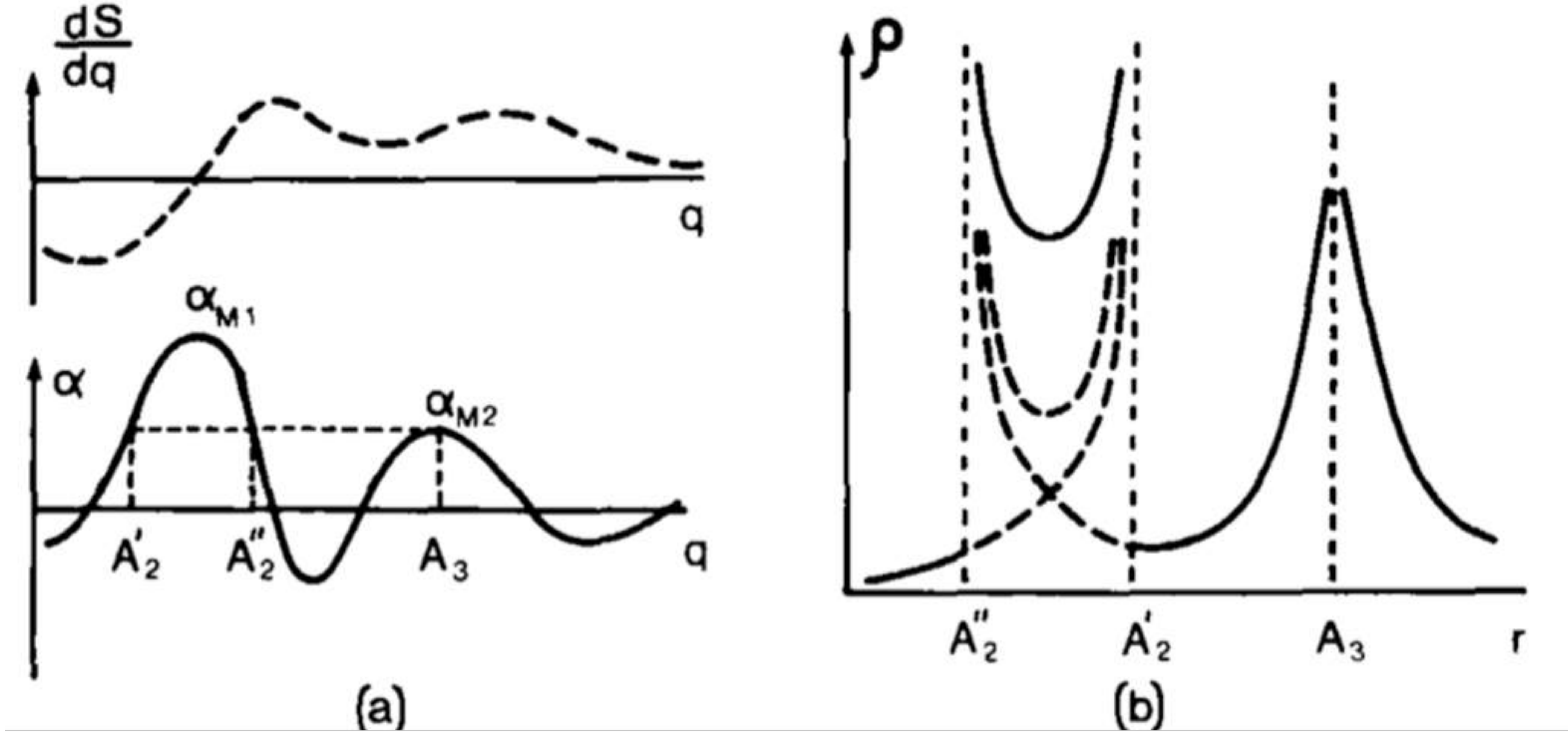

$$\rho_t(\mathbf{x}') = \sum_{\mathbf{q} \in \mathbf{x}_t^{-1}(\mathbf{x}')} \frac{\bar{\rho}}{|\det \nabla \mathbf{x}_t(\mathbf{q})|} = \sum_{\mathbf{q} \in \mathbf{x}_t^{-1}(\mathbf{x}')} \frac{\bar{\rho}}{|1+\mu_1(\mathbf{q})||1+\mu_2(\mathbf{q})||1+\mu_3(\mathbf{q})|}$$

with the eigenvalues of the deformation tensor $\nabla \mathbf{s}_t(\mathbf{q}) \mathbf{v}_i(\mathbf{q}) = \mu_i(\mathbf{q}) \mathbf{v}_i(\mathbf{q})$

Caustic conditions

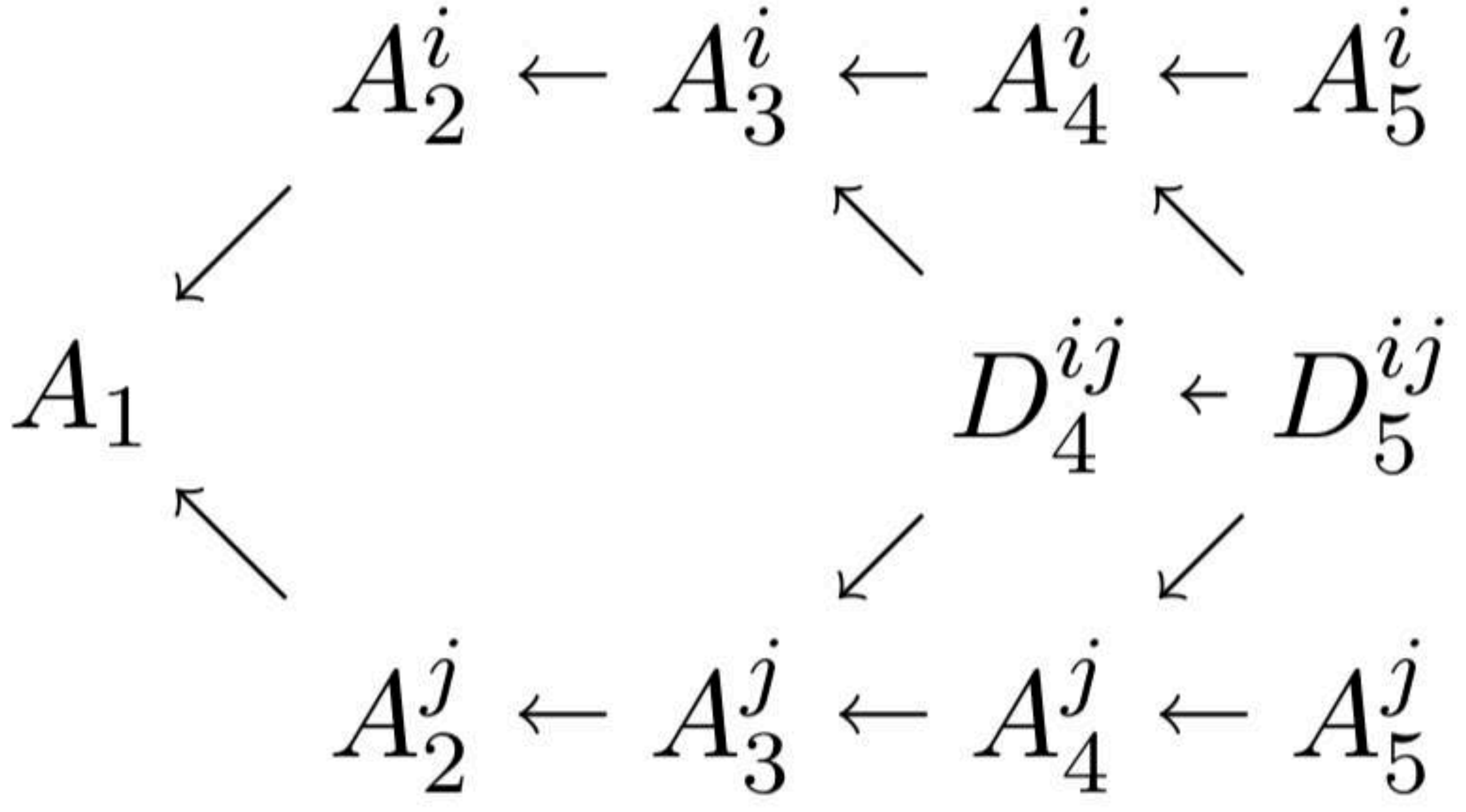

Iterative application of the shell-crossing condition

$$(1 + \mu_{it}(q_s))v_{it}^*(q_s) \cdot T = 0$$

leads to the caustic conditions on both the eigenvalue and eigenvector fields:

Fold:	$A_2^i(t) = \{\mathbf{q} \in L \mid 1 + \mu_{it}(\mathbf{q}) = 0\}$
Cusp:	$A_3^i(t) = \{\mathbf{q} \in L \mid \mathbf{q} \in A_2^i(t), \mathbf{v}_i \cdot \nabla \mu_{it} = 0\}$
Swallowtail:	$A_4^i(t) = \{\mathbf{q} \in L \mid \mathbf{q} \in A_3^i(t), \mathbf{v}_i \cdot \nabla(\mathbf{v}_i \cdot \nabla \mu_{it}) = 0\}$
Butterfly:	$A_5^i(t) = \{\mathbf{q} \in L \mid \mathbf{q} \in A_4^i(t), \mathbf{v}_i \cdot \nabla(\mathbf{v}_i \cdot \nabla(\mathbf{v}_i \cdot \nabla \mu_{it})) = 0\}$
Umbilic:	$D_4^{ij}(t) = \{\mathbf{q} \in L \mid 1 + \mu_{it}(\mathbf{q}) = 1 + \mu_{jt}(\mathbf{q}) = 0\}$
Parabolic:	$D_5^{ij}(t) = \{\mathbf{q} \in L \mid q \in D_4^{ij}(t), \mathbf{v}_i \cdot \nabla \mu_i = \mathbf{v}_j \cdot \nabla \mu_j = 0\}$

Morse-Smale theory of full deformation tensor field. No free parameters!

Feldbrugge et al (2019)

Caustic conditions

Singularity class	Singularity name	Feature in the 2D cosmic web	Feature in the 3D cosmic web	Profile $\rho(r)$
A_2	fold	collapsed region	collapsed region	$\rho(r) \propto r^{-1/2}$
A_3	cusp	filament	wall or membrane	$\rho(r) \propto r^{-2/3}$
A_4	swallowtail	cluster or knot	filament	$\rho(r) \propto r^{-3/4}$
A_5	butterfly	not stable	cluster or knot	$\rho(r) \propto r^{-4/5}$
D_4	hyperbolic/elliptic	cluster or knot	filament	$\rho(r) \propto r^{-1}$
D_5	parabolic	not stable	cluster or knot	$\rho(r) \propto r^{-1} \log(1/r)$

The identification of the different caustics in the 2- and 3-dimensional cosmic web

Feldbrugge et al (2019)

The geometry of the cosmic web

Caustic conditions

Note that:

- The **eigenvalue and eigenvector** fields are **non-linear transformations of the density perturbations**
- The web-like nature is embedded in the distribution of the **eigenvalue** *and* **eigenvector fields**

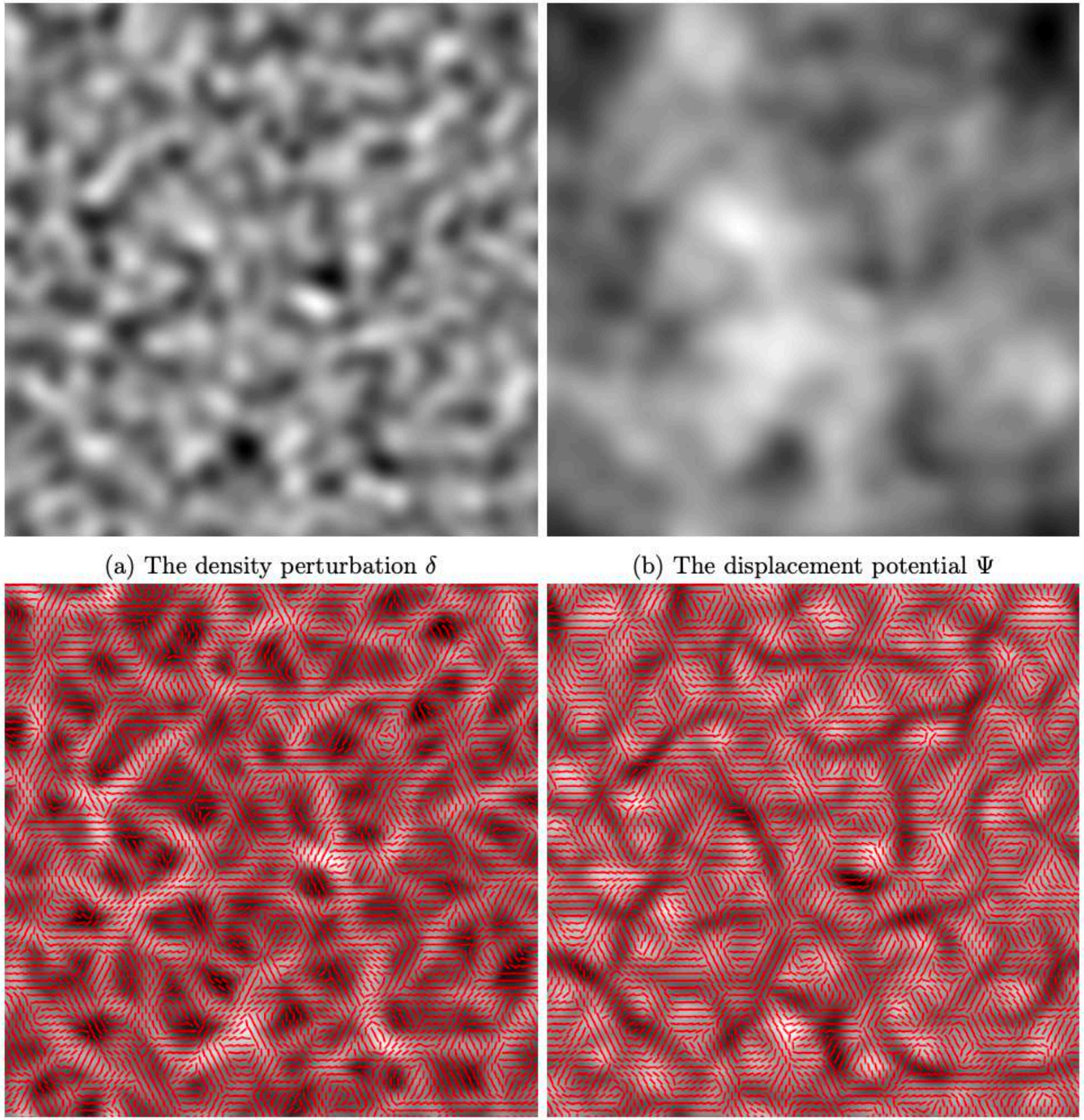

(a) The density perturbation δ

(b) The displacement potential Ψ

(c) The first eigenvalue and eigenvector fields λ_1, and $\boldsymbol{v}_1$

(d) The second eigenvalue and eigenvector fields λ_2, and $\boldsymbol{v}_2$

Caustic conditions

$\mathbf{x}_t(\mathbf{q}) = \mathbf{q} - b_+(t)\,\nabla\Psi(\mathbf{q})$

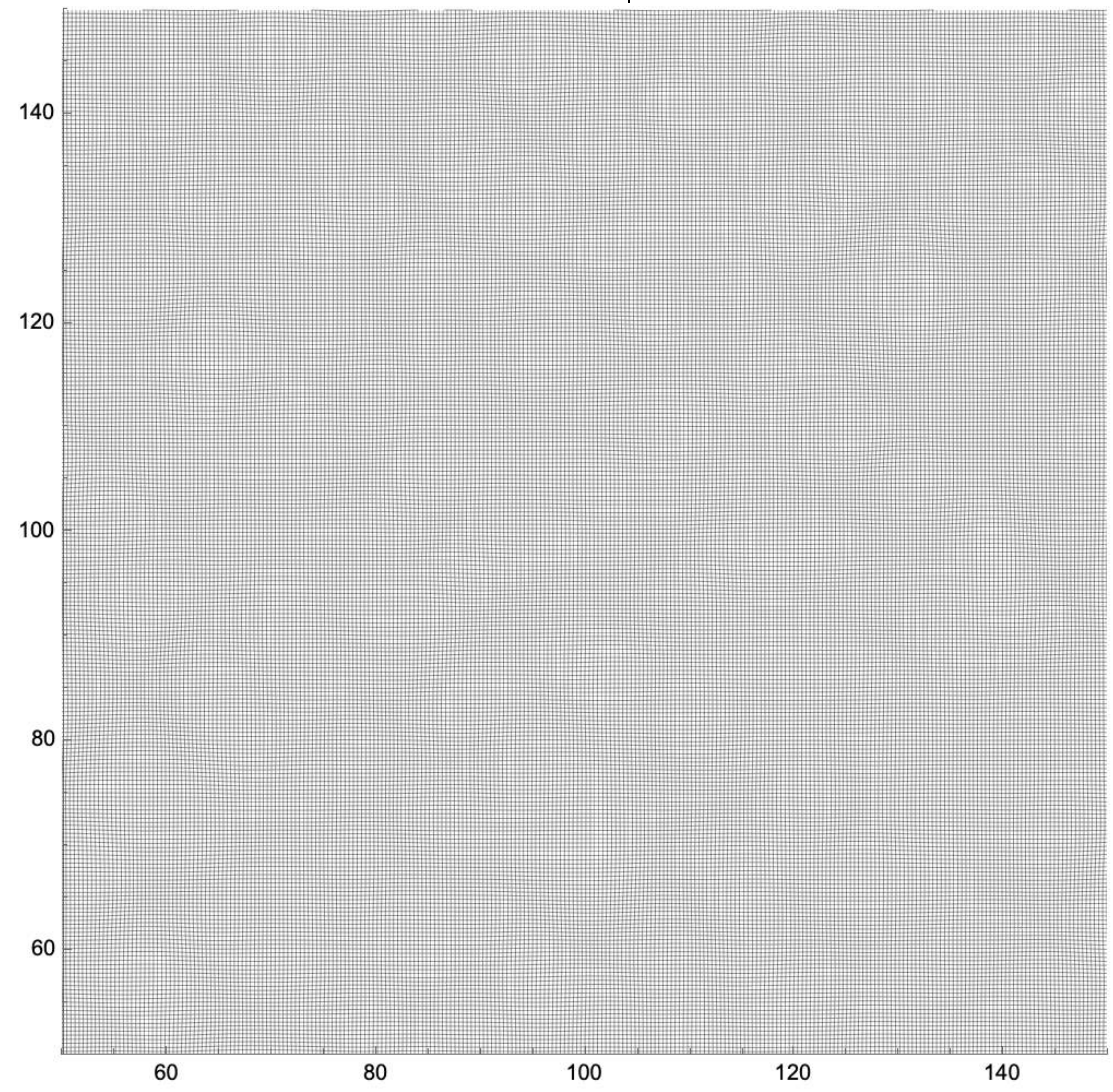

$\mathbf{x}_t(\mathbf{q}) = \mathbf{q} + \mathbf{s}_t(\mathbf{q})$

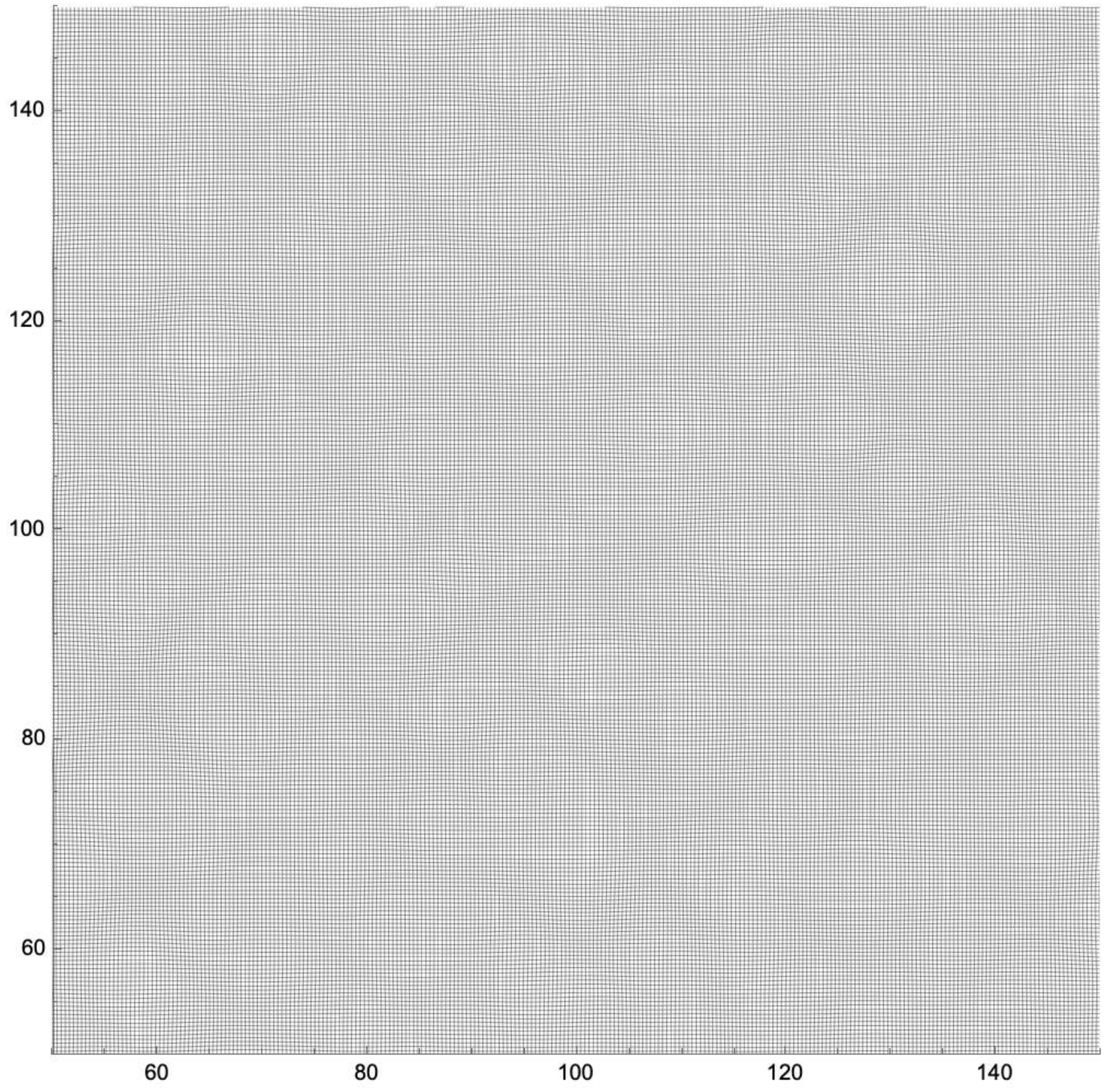

Caustic conditions

$\mathbf{x}_t(\mathbf{q}) = \mathbf{q} - b_+(t)\,\nabla\Psi(\mathbf{q})$

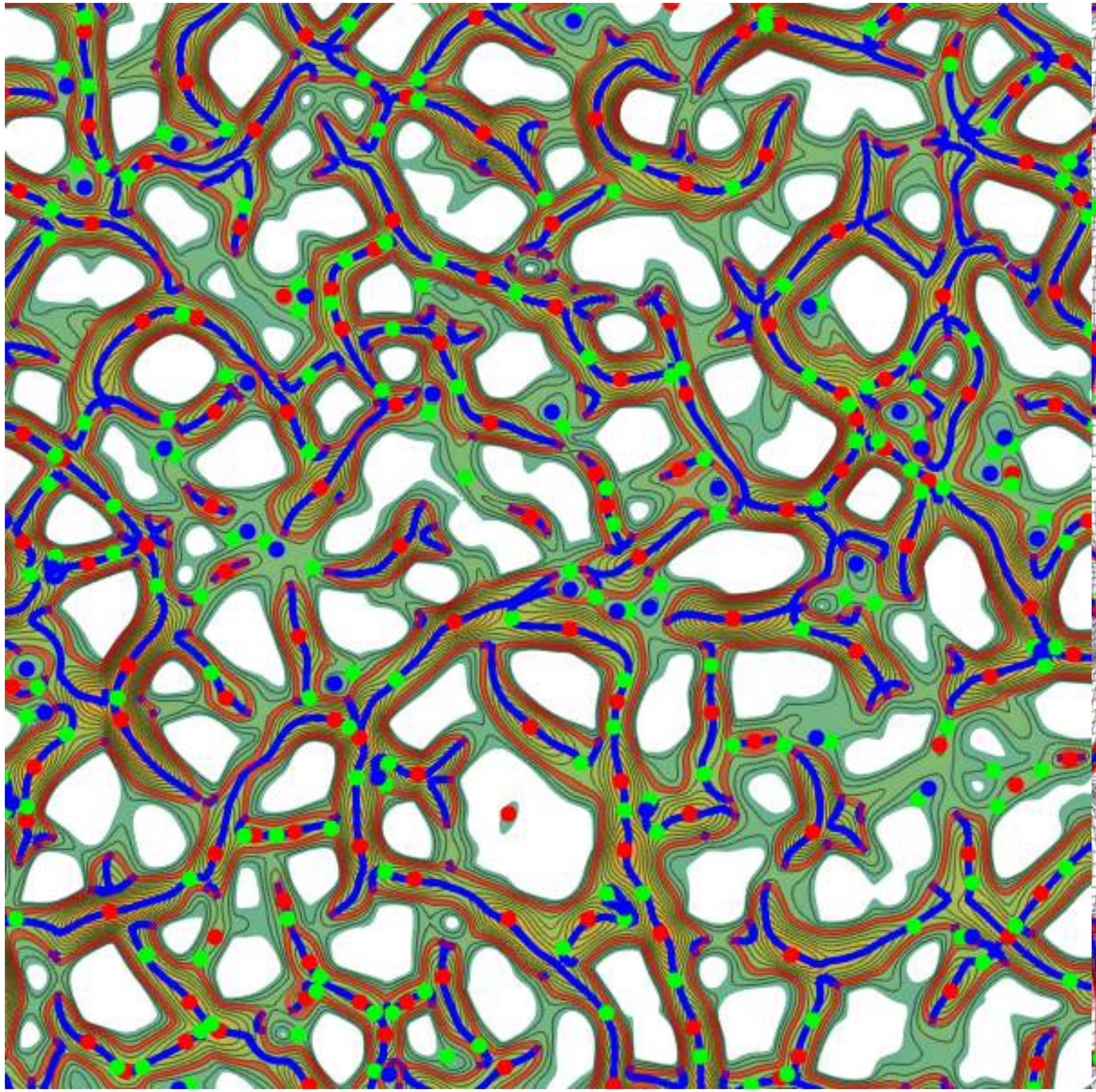

$\mathbf{x}_t(\mathbf{q}) = \mathbf{q} + \mathbf{s}_t(\mathbf{q})$

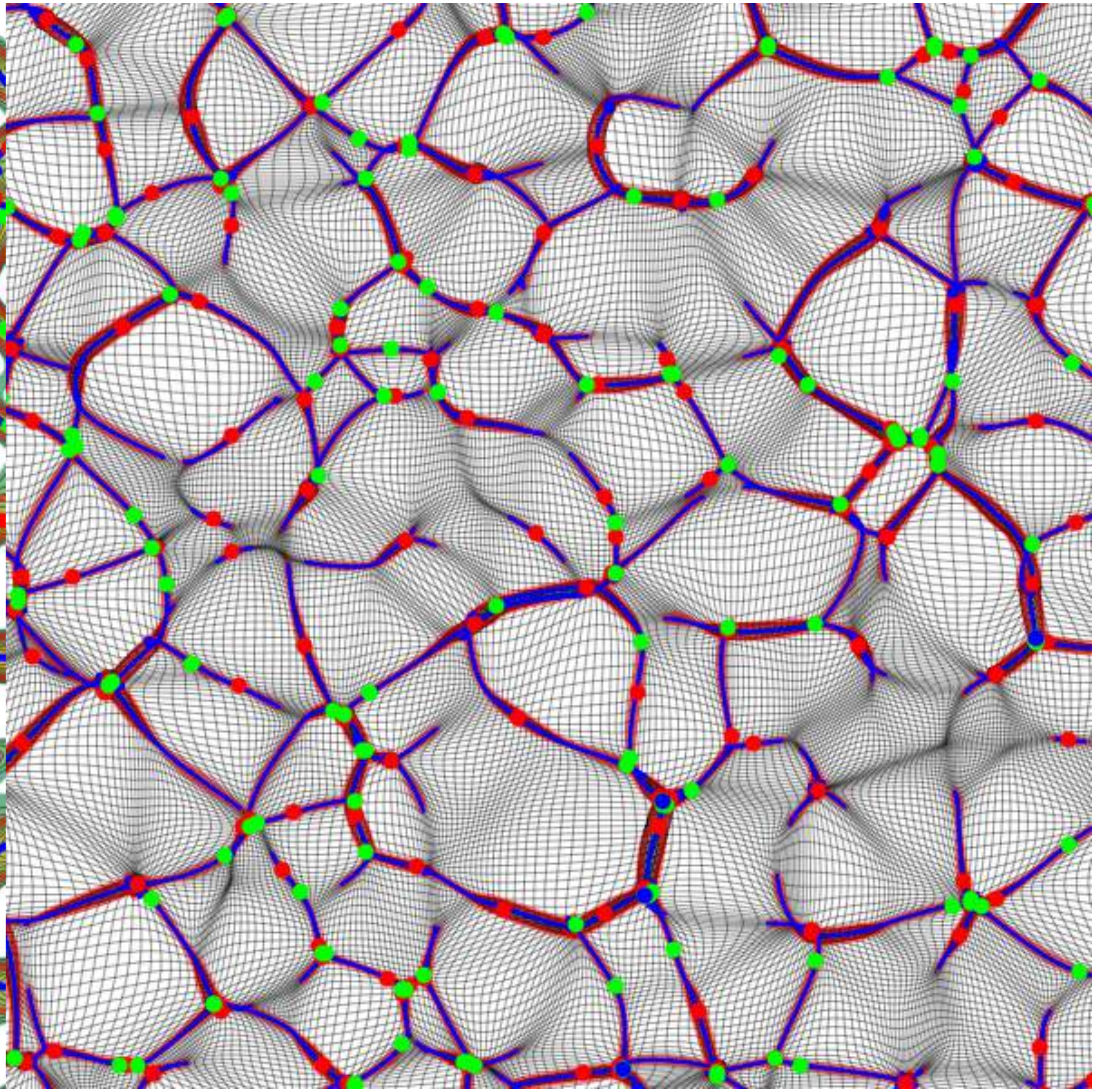

Caustic conditions

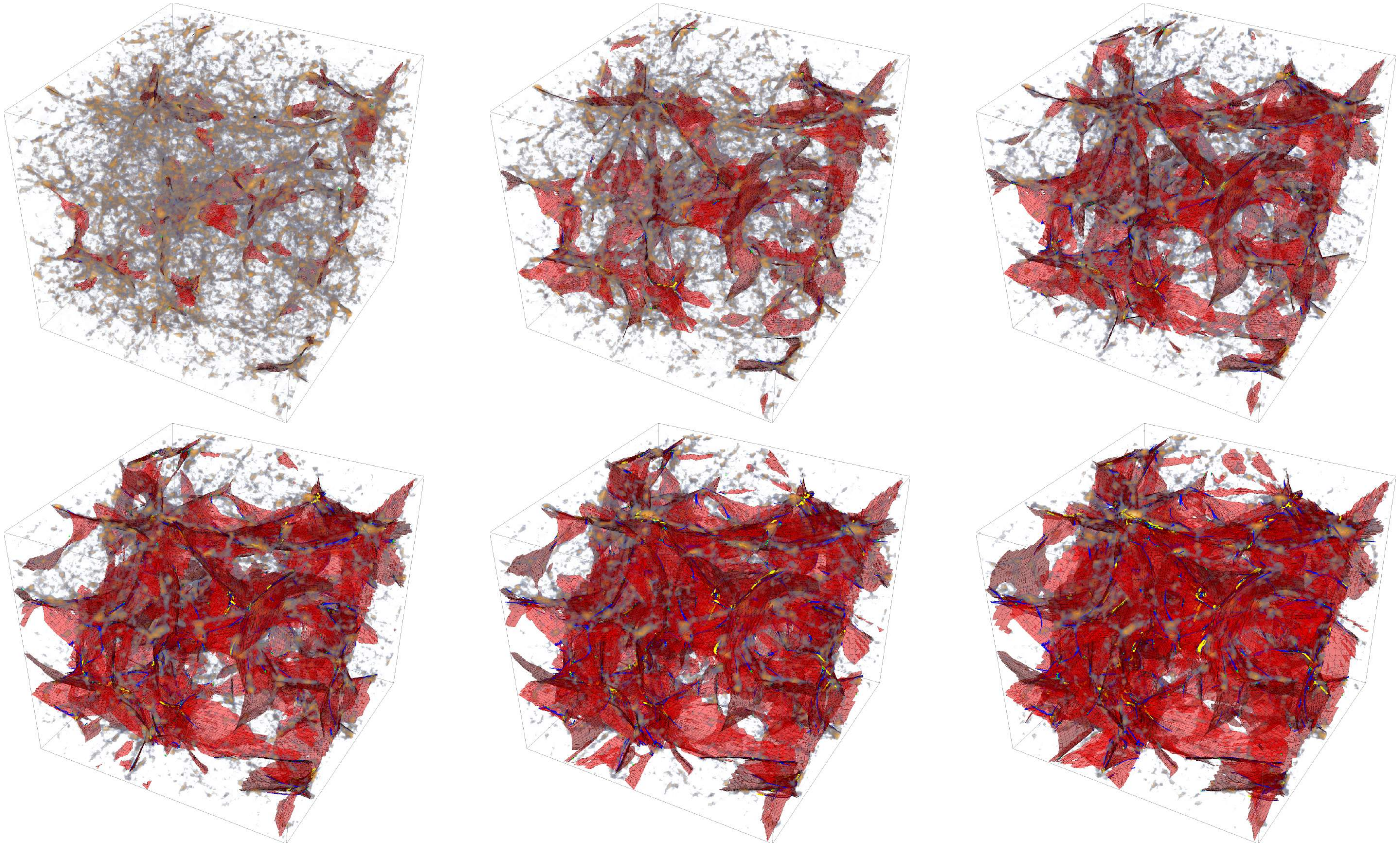

Non-linear constrained GRFs

Gaussian random field

The cosmological initial conditions are often modelled by a Gaussian random field, which is an stochastic process:

$$P[f \in \mathcal{S}] = \mathcal{N} \int \mathbf{1}_{\mathcal{S}}(f) e^{-S[f]} \mathcal{D}f$$

with the 'action'

$$S[f] \equiv \frac{1}{2} \iint [f(\boldsymbol{q}_1) - \bar{f}(\boldsymbol{q}_1)] K(\boldsymbol{q}_1, \boldsymbol{q}_2) [f(\boldsymbol{q}_2) - \bar{f}(\boldsymbol{q}_2)] \mathrm{d}\boldsymbol{q}_1 \mathrm{d}\boldsymbol{q}_2,$$

where the kernel is the inverse of the two-point correlation function

$$\int K(\boldsymbol{q}_1, \boldsymbol{q}) \xi(\boldsymbol{q}, \boldsymbol{q}_2) \mathrm{d}\boldsymbol{q} = \delta_D^{(2)}(\boldsymbol{q}_1 - \boldsymbol{q}_2)$$

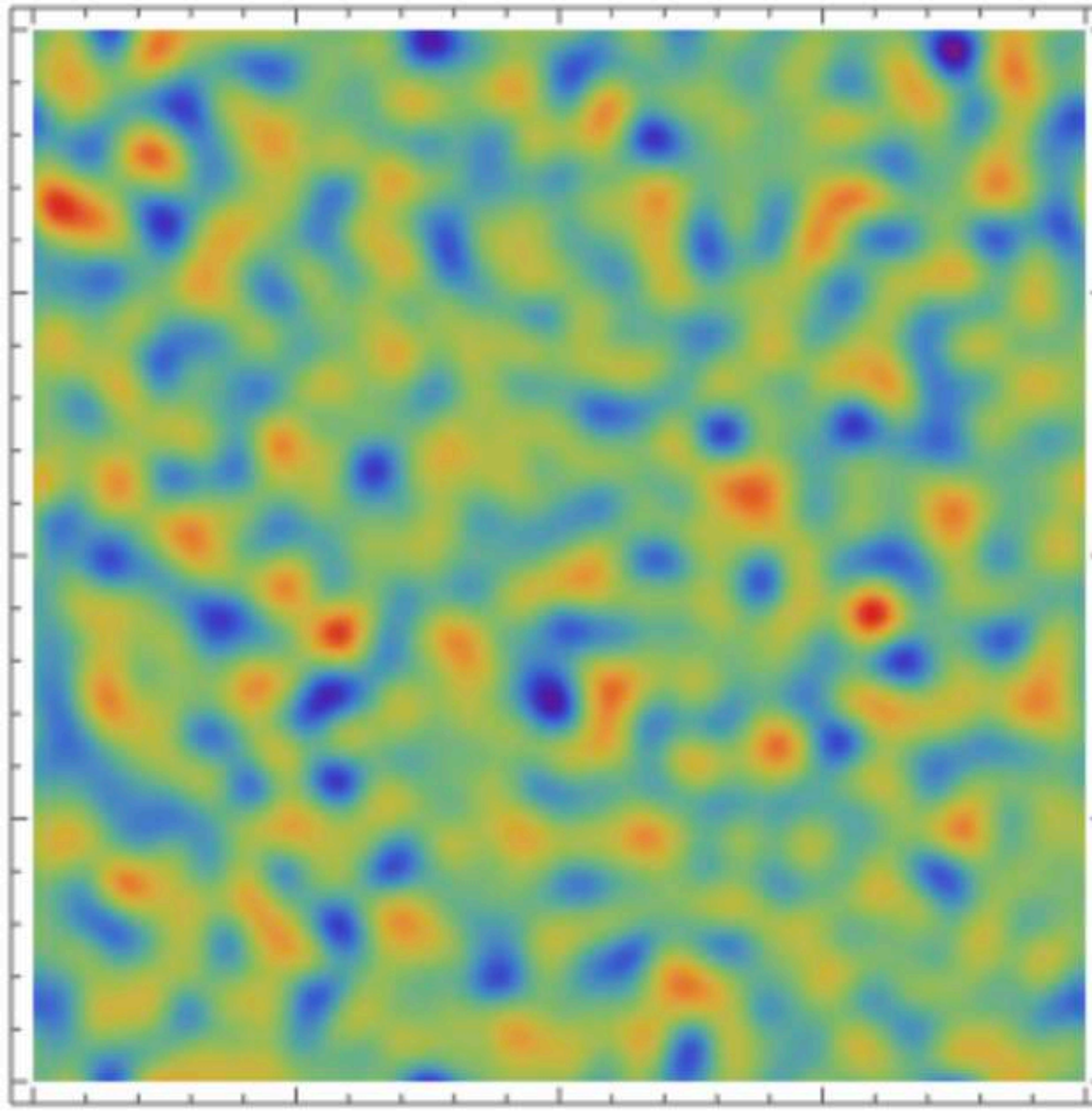

Linear constrained GRFs

We construct constrained simulations by adding constraints to the initial conditions

For linear constraints, the residue is independent of the value that the constraints assume:

$$\mathbf{x} = (\mathbf{x}_1, \mathbf{x}_2) \quad \mu = (\mu_1, \mu_2) \quad \Sigma = \begin{pmatrix} \Sigma_{11} & \Sigma_{12} \\ \Sigma_{21} & \Sigma_{22} \end{pmatrix}$$

when imposing $\mathbf{x}_2 = \mathbf{a}$ the constrained distribution is Gaussian with

$$\bar{\mu} = \mu_1 + \Sigma_{12}\Sigma_{22}^{-1}(\mathbf{a} - \mu_2) \qquad \bar{\Sigma} = \Sigma_{11} - \Sigma_{12}\Sigma_{22}^{-1}\Sigma_{21}$$

note that $\bar{\Sigma}$ is independent of $\mathbf{a}$

Bertschinger 1987
Hoffman, Ribak 1991
van de Weygaert & Bertschinger 1996
Log-normal: Ravi Sheth 1997

Non-linear constraints

- The eigenvalue and eigenvector fields are not Gaussian, and the caustic conditions are non-linear. For this reason, we develop non-linear constraint Gaussian random field theory

$$\mathcal{M}_{\mathcal{C}} = \{\boldsymbol{c} \,|\, \mathcal{C}_i(\boldsymbol{c}) = 0 \text{ for all } i = 1, \dots, N\}.$$

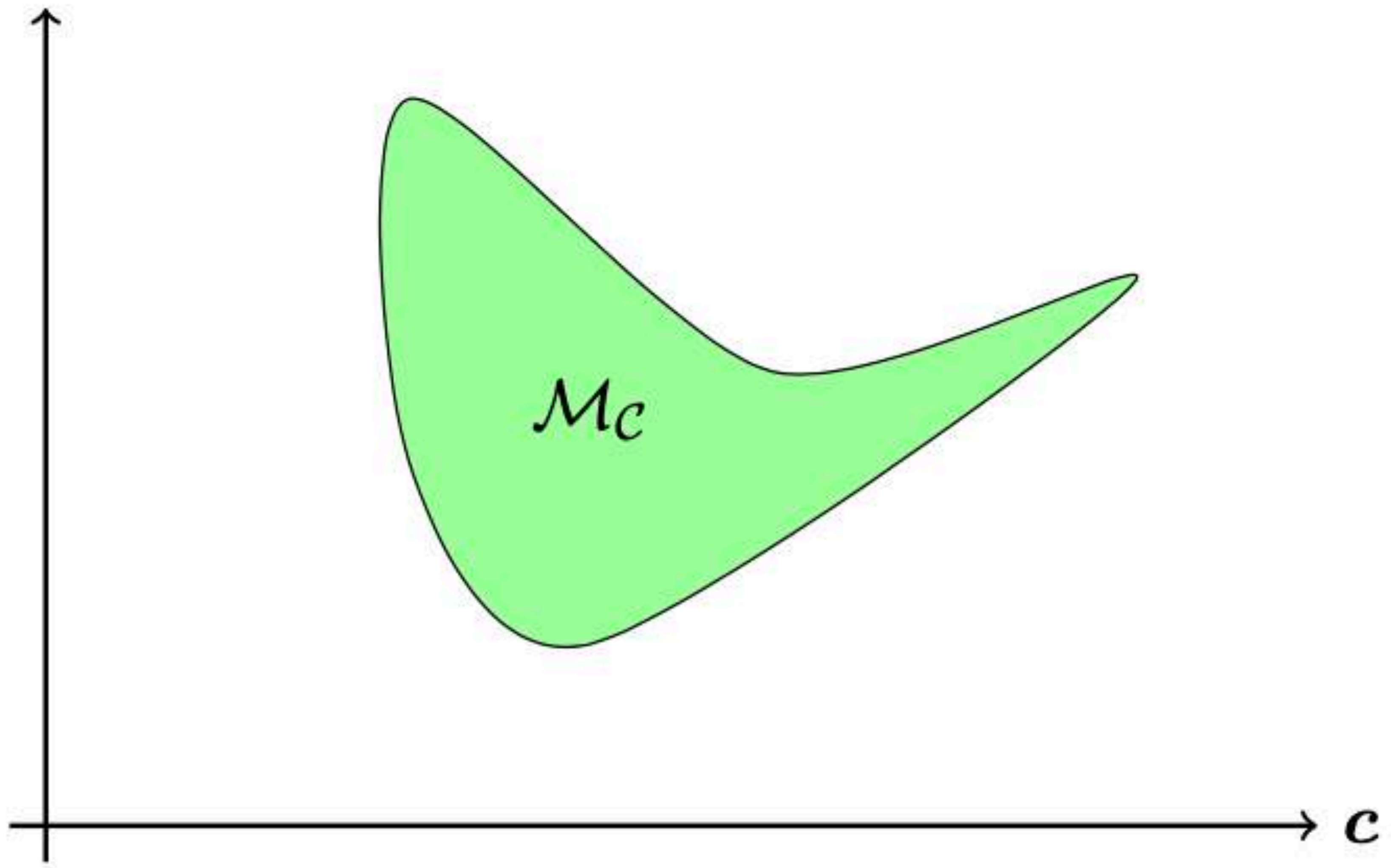

- On this constraint manifold, we find the induced probability density

$$p(\boldsymbol{c} \,|\, \boldsymbol{c} \in \mathcal{M}_{\mathcal{C}}) = \frac{p(\boldsymbol{c})}{\int_{\mathcal{M}_{\mathcal{C}}} p(\boldsymbol{c})\, \mathrm{d}\boldsymbol{c}}\,.$$

Feldbrugge and Weygaert (2023)

What makes a wall/filament?

JF and van de Weygaert 2024

Cusp filament (2D)

Candidate condition:

$$\lambda_1 = 1/b_+(t_c) \quad \mathbf{v}_1 \cdot \nabla \lambda_1 = 0$$

$$\mathbf{n} = \nabla(\mathbf{v}_1 \cdot \nabla \lambda_1)$$

Unsatisfactory as:

1. Points in Eulerian space **biased towards clusters**

2. Zel'dovich approximation **invalid in clusters**

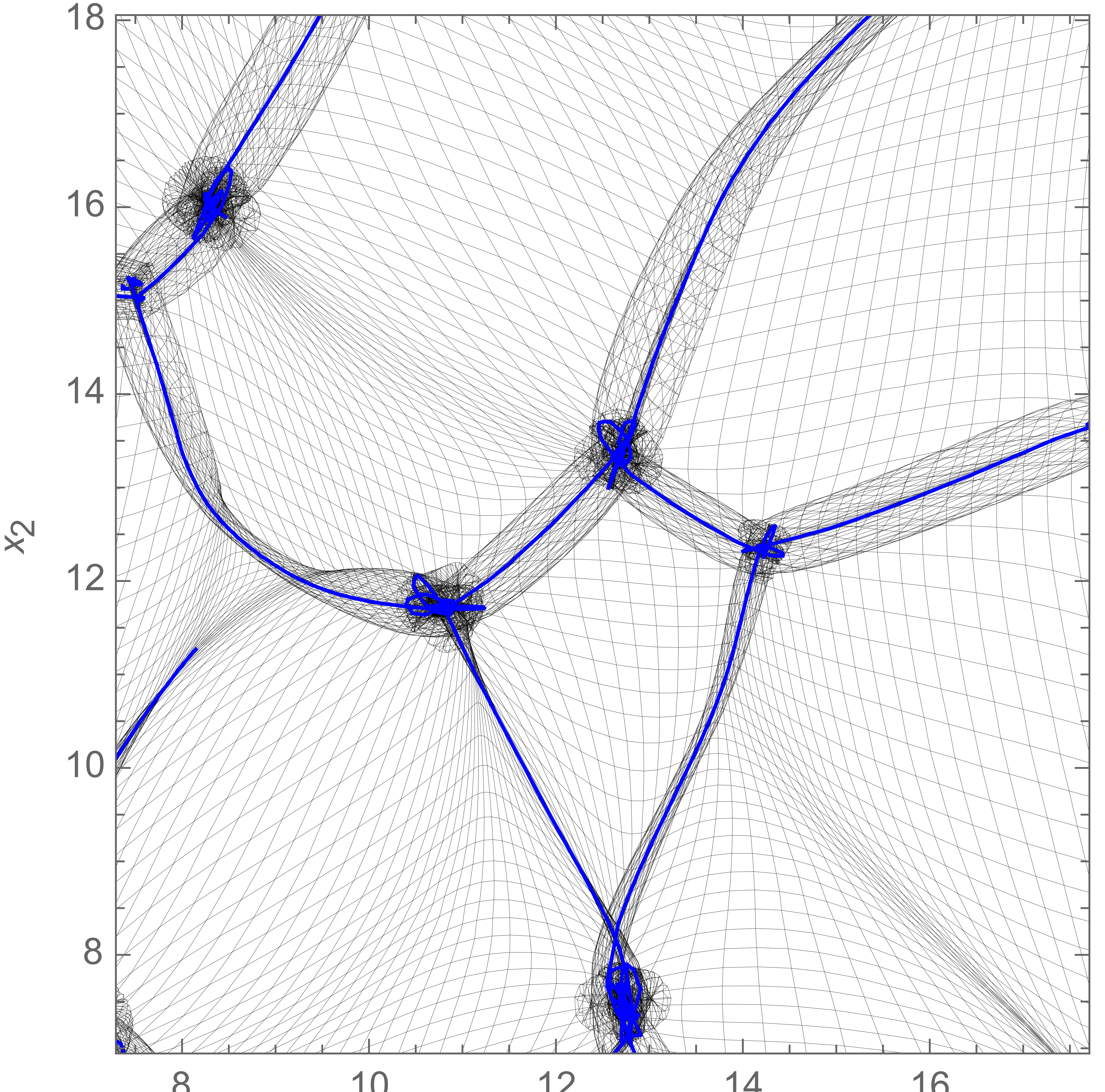

Cusp filament (2D)

Require that the cusp line is **maximally expanding along the direction of the filament**

$$\lambda_1 = 1/b_+(t_c) \qquad \lambda_2 < 0$$
$$\mathbf{v}_1 \cdot \nabla \lambda_1 = 0 \qquad \mathbf{v}_2 \cdot \nabla \lambda_2 = 0$$
$$\mathbf{n} = \nabla(\mathbf{v}_1 \cdot \nabla \lambda_1) \qquad \mathbf{v}_2[\mathscr{H}\lambda_2]\mathbf{v}_2 > 0$$

Note the **symmetry** between the first and second eigenvalue fields!

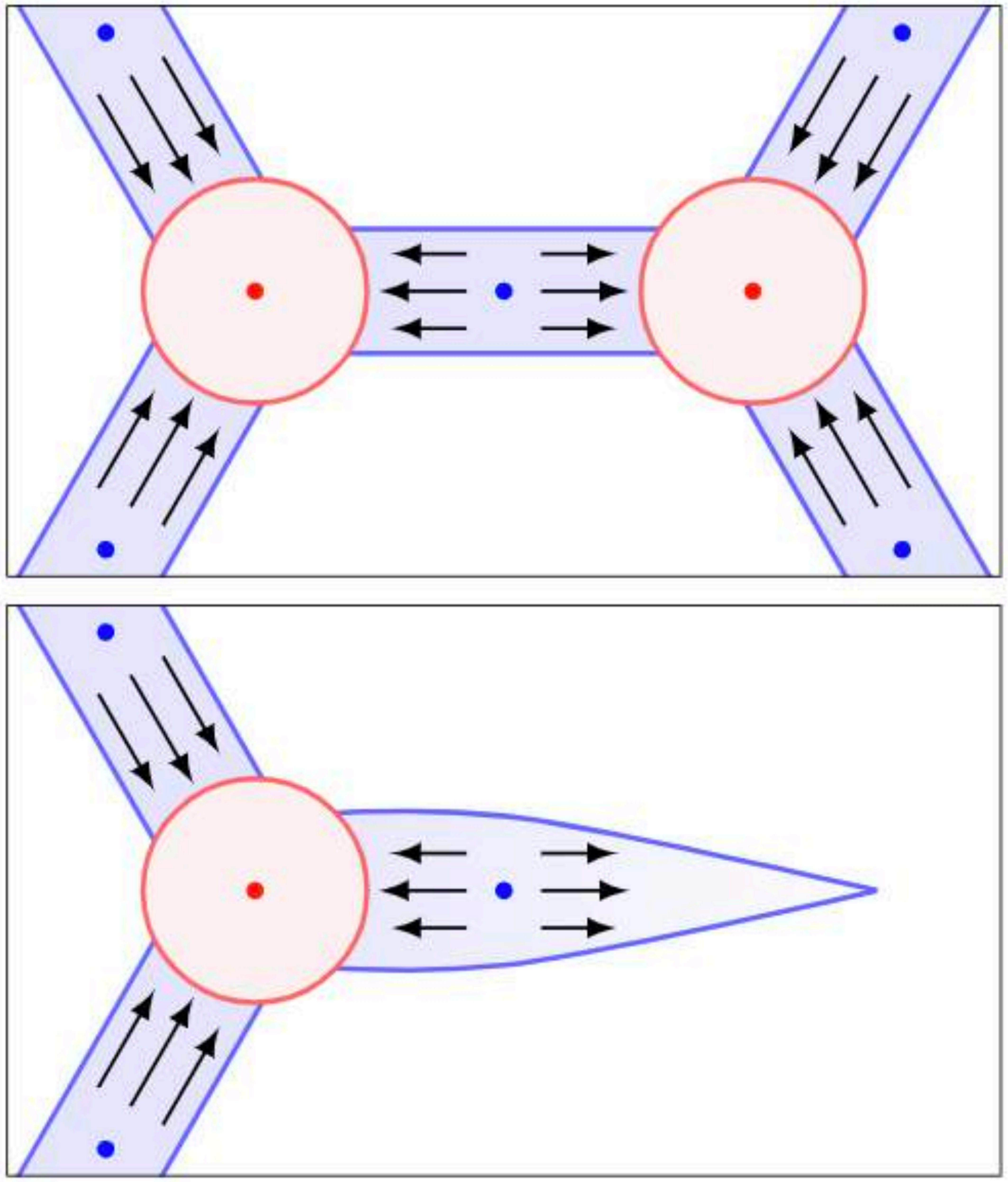

Cusp filament (2D)

Require that the cusp line is **maximally expanding along the direction of the filament**

$$\lambda_1 = 1/b_+(t_c) \qquad \lambda_2 < 0$$
$$\mathbf{v}_1 \cdot \nabla \lambda_1 = 0 \qquad \mathbf{v}_2 \cdot \nabla \lambda_2 = 0$$
$$\mathbf{n} = \nabla(\mathbf{v}_1 \cdot \nabla \lambda_1) \qquad \mathbf{v}_2[\mathscr{H}\lambda_2]\mathbf{v}_2 > 0$$

Note the **symmetry** between the first and second eigenvalue fields!

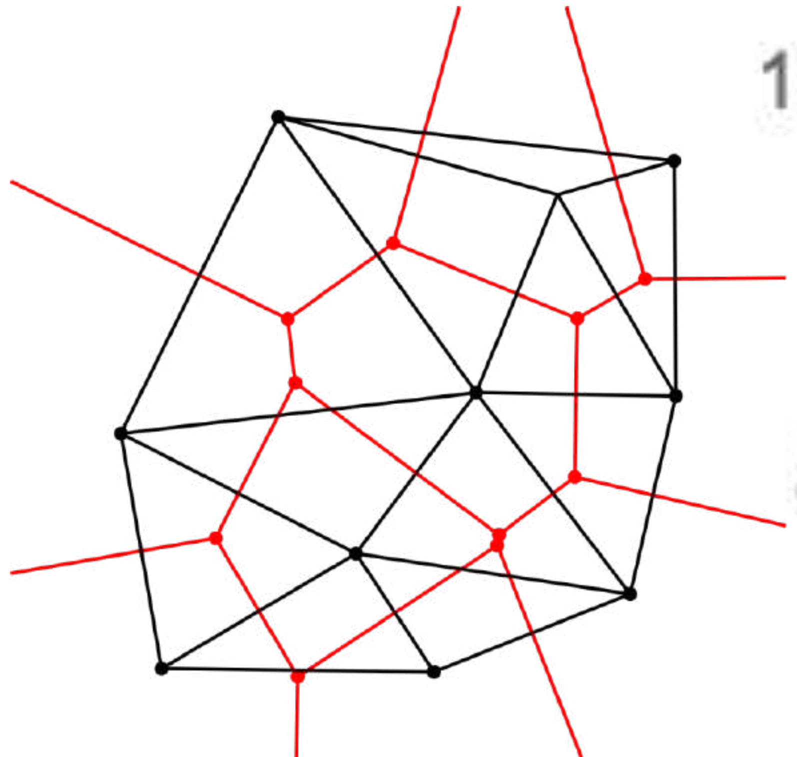

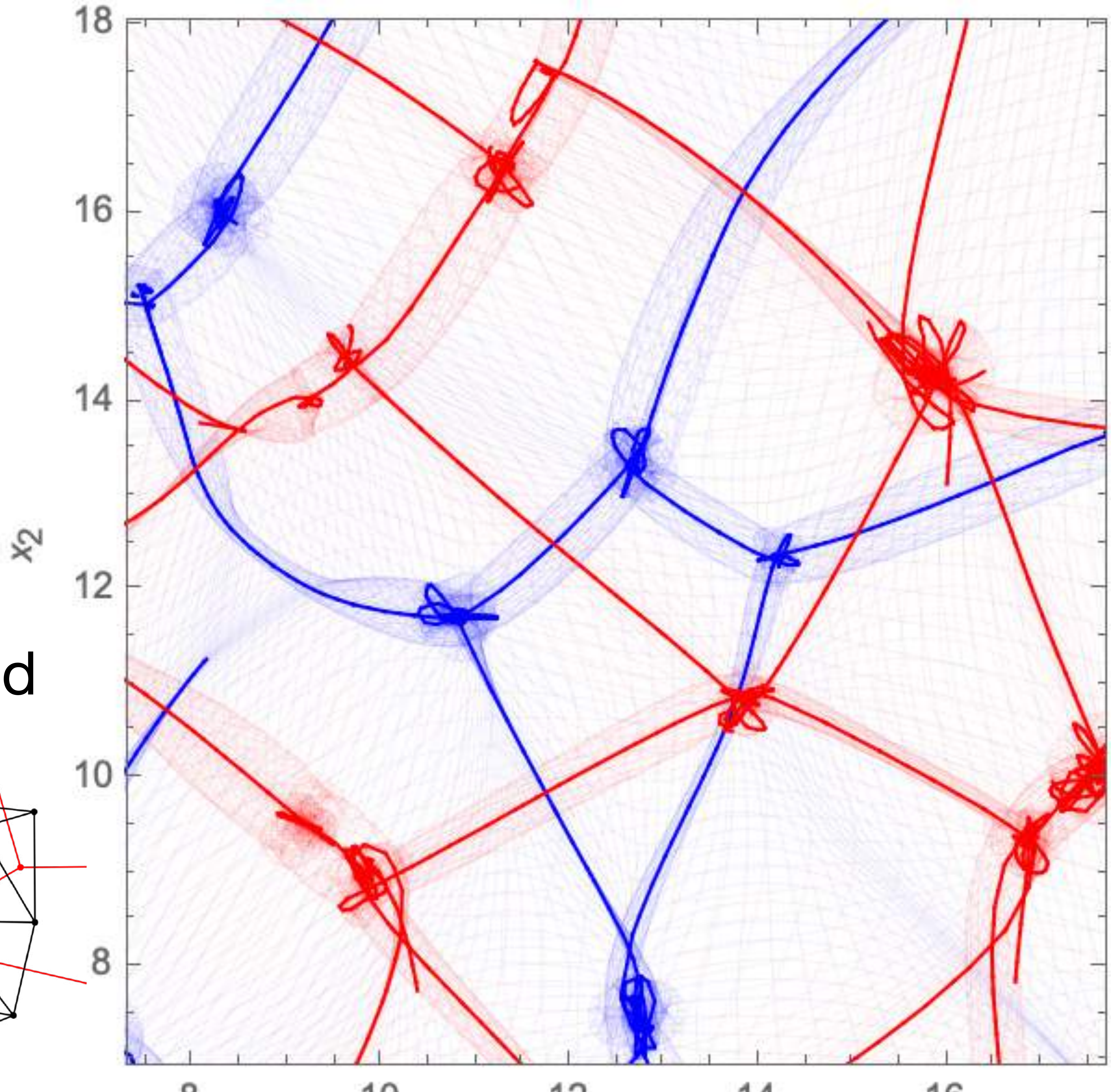

Cusp filament (2D)

After sampling the non-Gaussian distribution of the derivative of the primordial destitution in a point with an HMC algorithm,

$$\lambda_1 = 1/b_+(t_c) \qquad \lambda_2 < 0$$
$$\mathbf{v}_1 \cdot \nabla \lambda_1 = 0 \qquad \mathbf{v}_2 \cdot \nabla \lambda_2 = 0$$
$$\mathbf{n} = \nabla(\mathbf{v}_1 \cdot \nabla \lambda_1) \qquad \mathbf{v}_2[\mathscr{H}\lambda_2]\mathbf{v}_2 > 0$$

$$\Rightarrow \quad p(Y) \propto e^{-U(Y)}$$

we generate constrained initial conditions with the Hoffman-Ribak algorithm

See **Maé Rodriguez** for details!

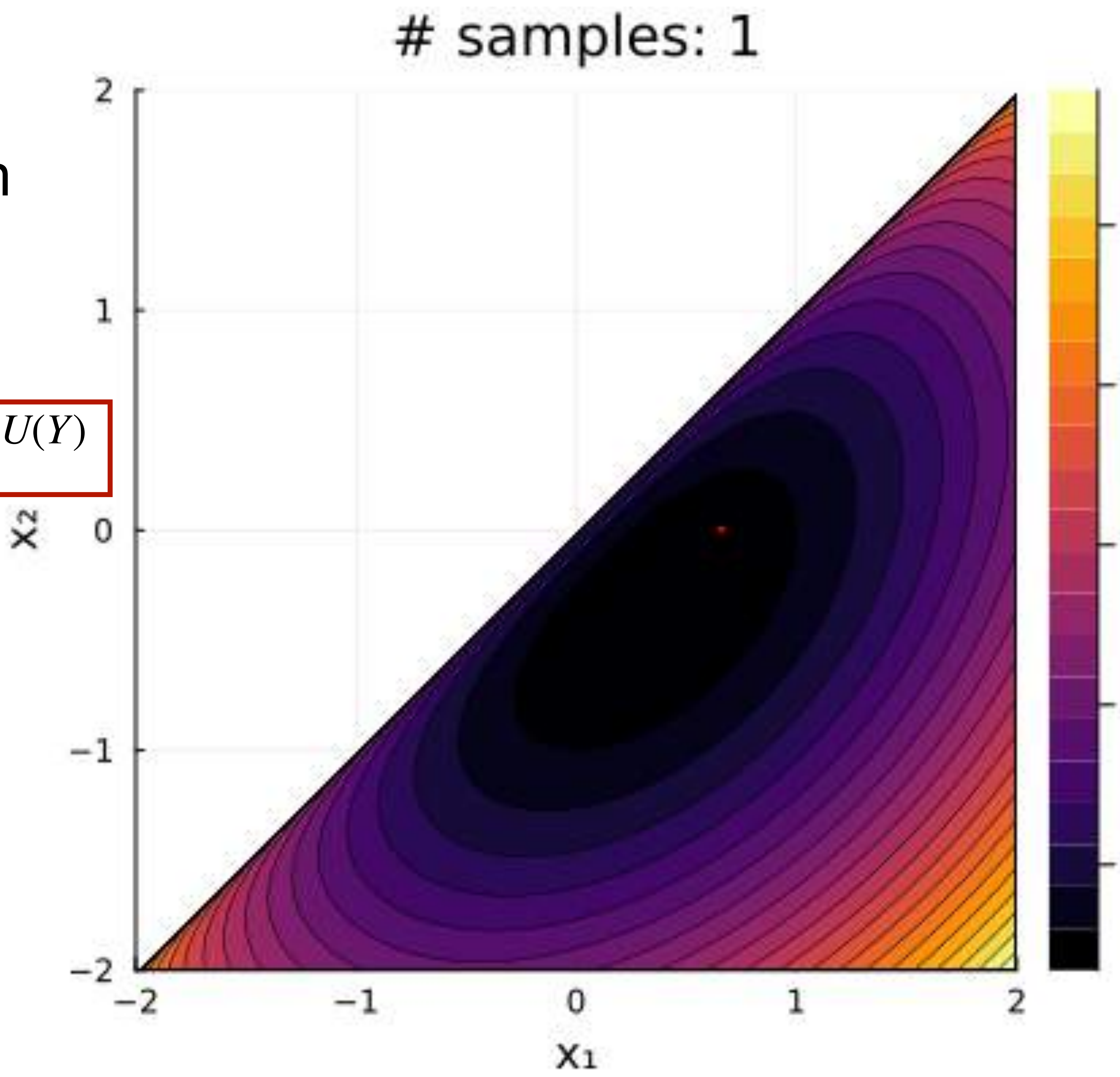

Cusp filament realizations

Specifying:

- **formation time,**
- **length scale,**
- and **orientation**

Dark matter
512 x 512 N-body
simulations

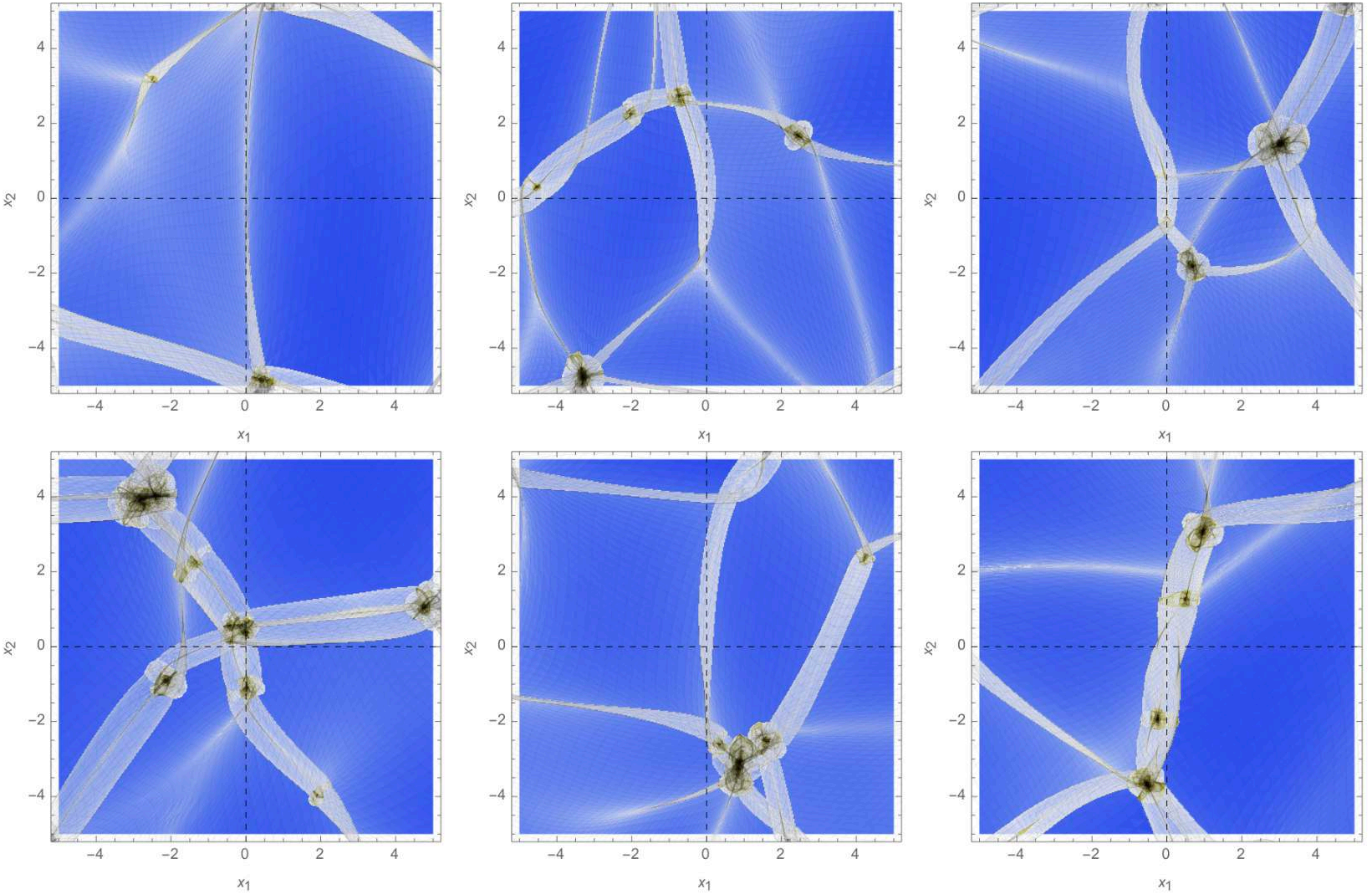

Median field

Cusp filaments

We run 1000 dark matter 512 x 512 N-body simulations, evaluate the density field and compute the median for every pixel

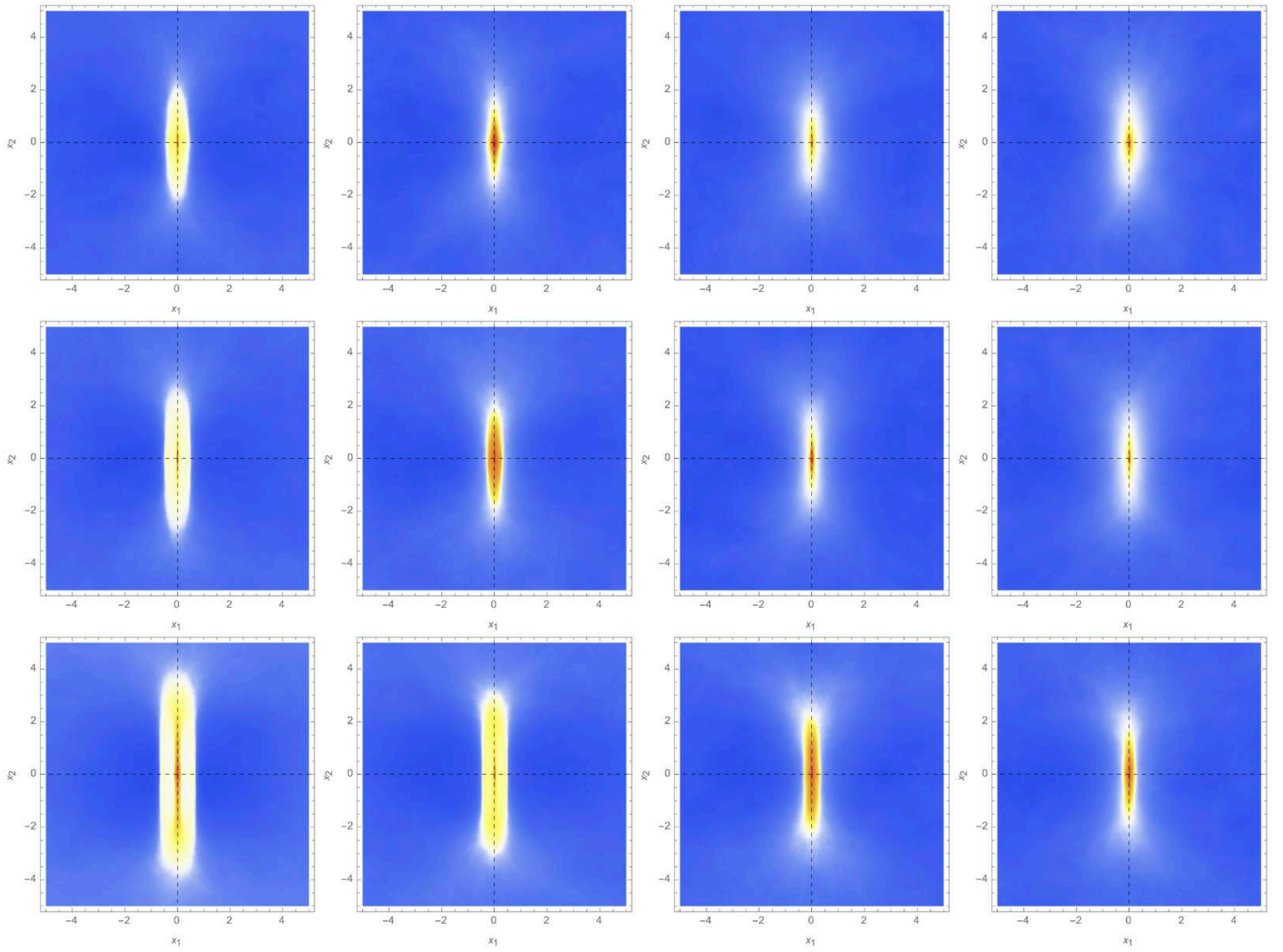

Cusp caustic (2D)

$$\lambda_1 = 1/b_+(t_c) \qquad \lambda_2 < 0$$
$$\mathbf{v}_1 \cdot \nabla \lambda_1 = 0 \qquad \mathbf{v}_2 \cdot \nabla \lambda_2 = 0$$
$$\mathbf{n} = \nabla(\mathbf{v}_1 \cdot \nabla \lambda_1) \qquad \mathbf{v}_2[\mathscr{H}\lambda_2]\mathbf{v}_2 > 0$$

Formation times and number densities

$$p(\textbf{center of filament forms a growing mode } b_c) = \frac{2\lambda_1^2 \Theta_H(\lambda_1)}{3\sigma_2^2}\left[2\lambda_1 e^{-\frac{4\lambda_1^2}{3\sigma_2^2}} \textbf{erfc}\left(\frac{\lambda_1}{\sqrt{6}\sigma_2}\right) + \sqrt{\frac{6}{\pi}}\sigma_2 e^{-\frac{3\lambda_1^2}{2\sigma_2^2}}\right]\Bigg|_{\lambda_1 = 1/b_c}$$

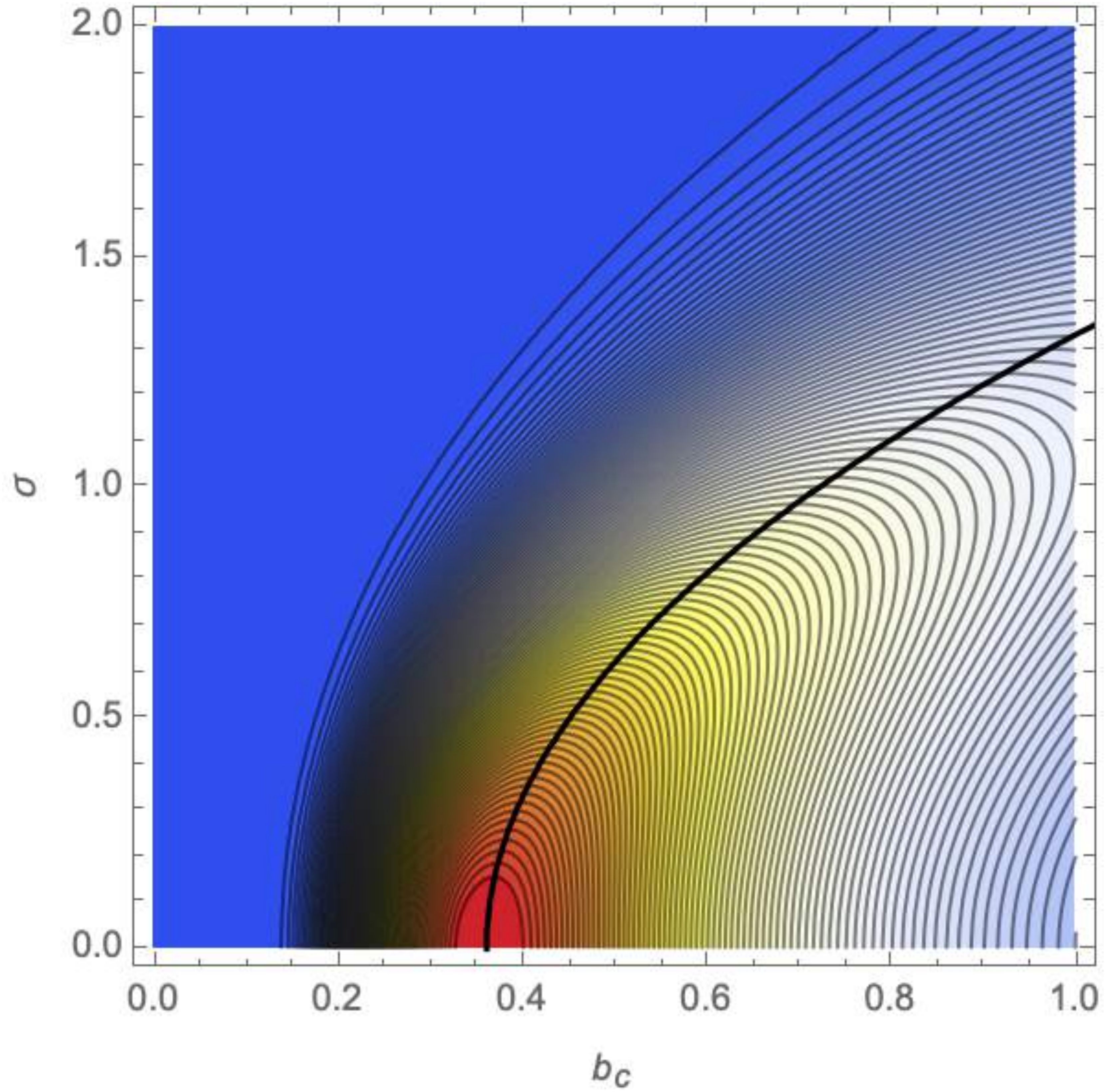

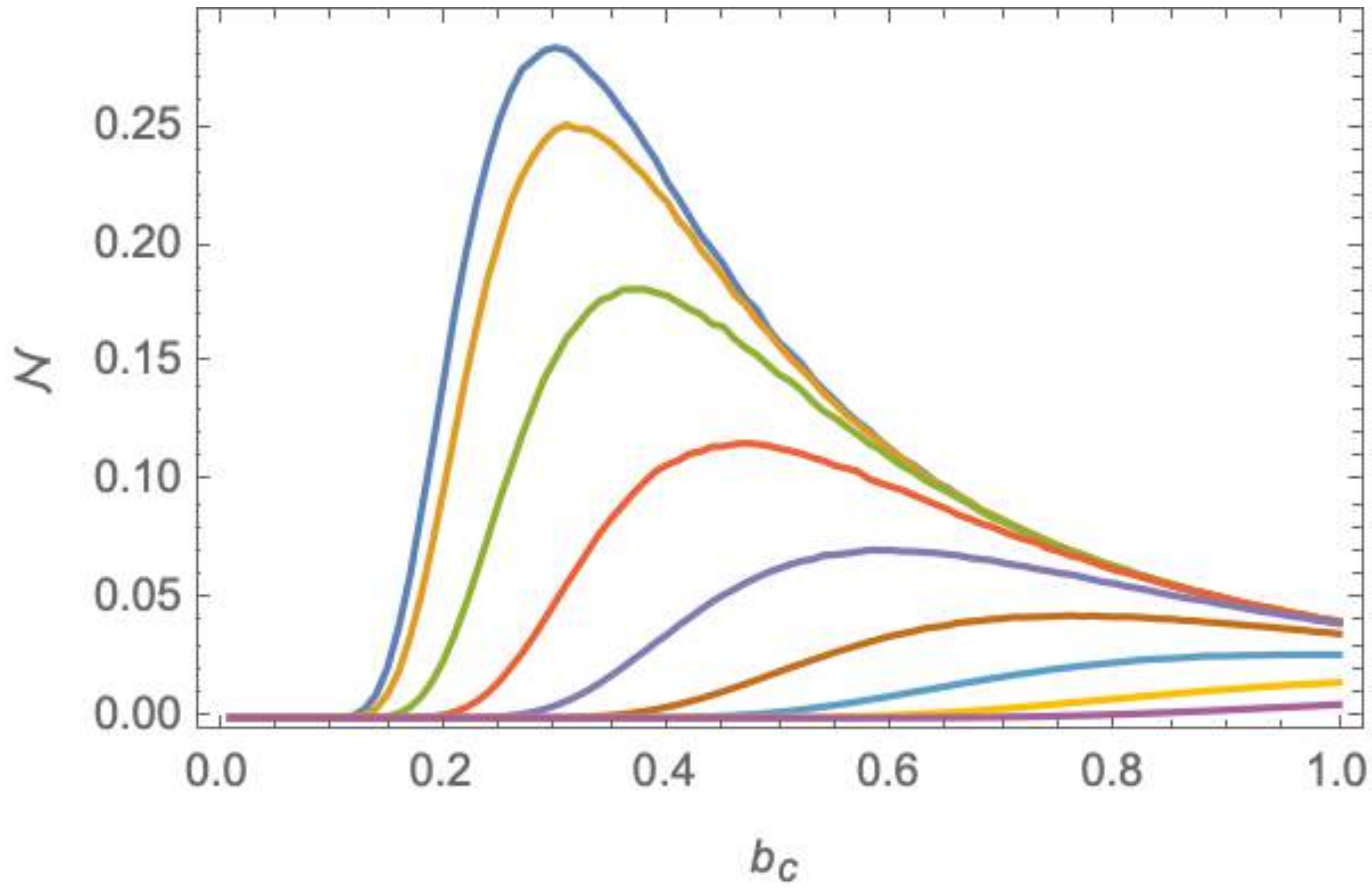

Saddle point in primordial fields

Saddle points in the primordial density and gravitational field specifying:

- **length scale**,
- and **orientation**

Dark matter
512 x 512 N-body simulations

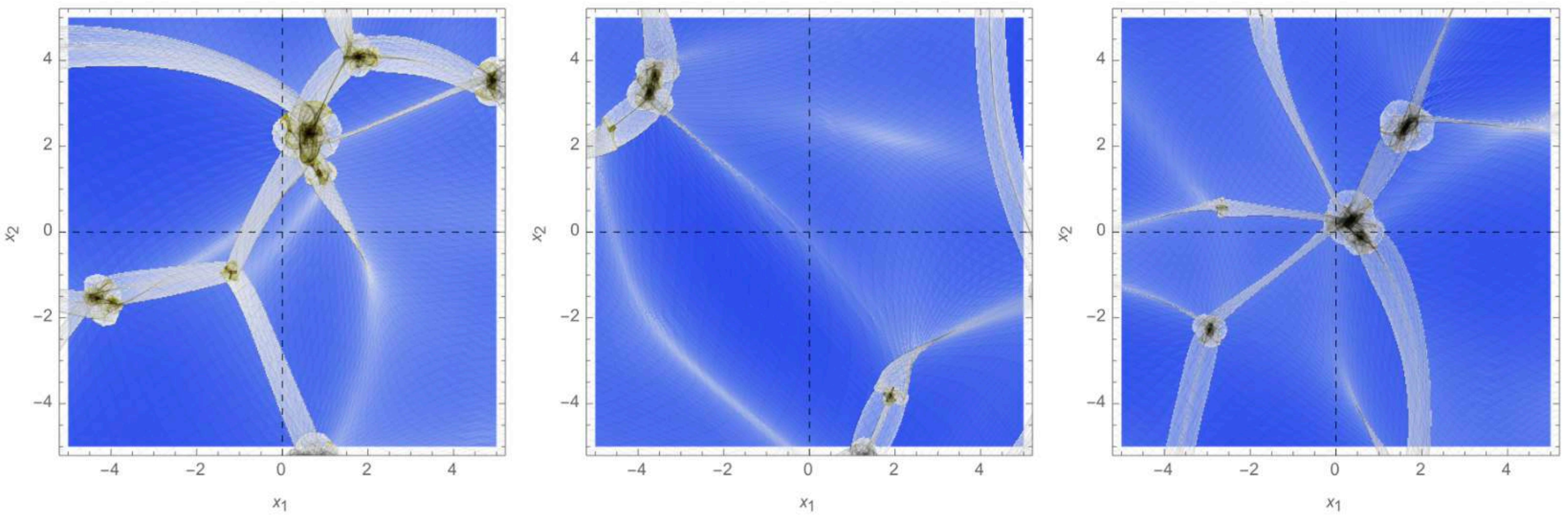

Figure 11. Realizations of saddle points in the smoothed primordial density perturbation at the scale $\sigma = 0.5$. We plot the N-body particles and the initial mesh on the corresponding density field $\log(\rho + 1)$.

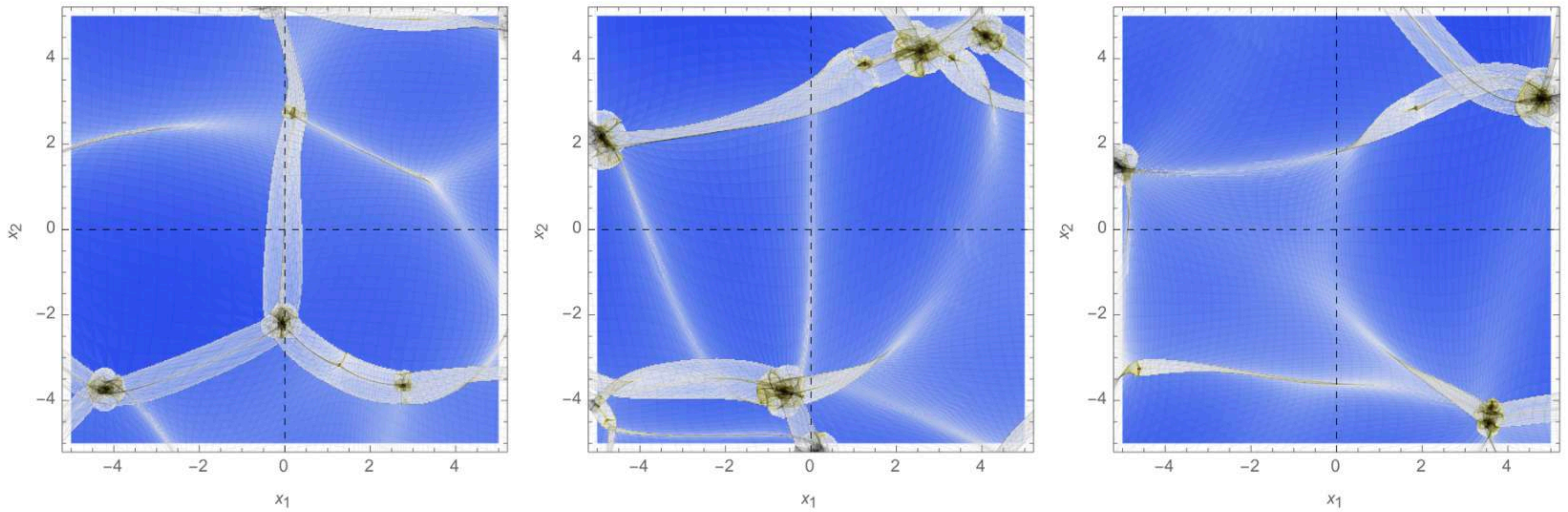

Figure 14. Realizations of saddle points in the smoothed primordial gravitational potential at the scale $\sigma = 0.5$. We plot the N-body particles and the initial mesh on the corresponding density field $\log(\rho + 1)$.

Median field

Saddle point filaments

We run 1000 dark matter 512 x 512 N-body simulations, evaluate the density field and compute the median for every pixel

Lengt scale

Density perturbation

Gravitational potential

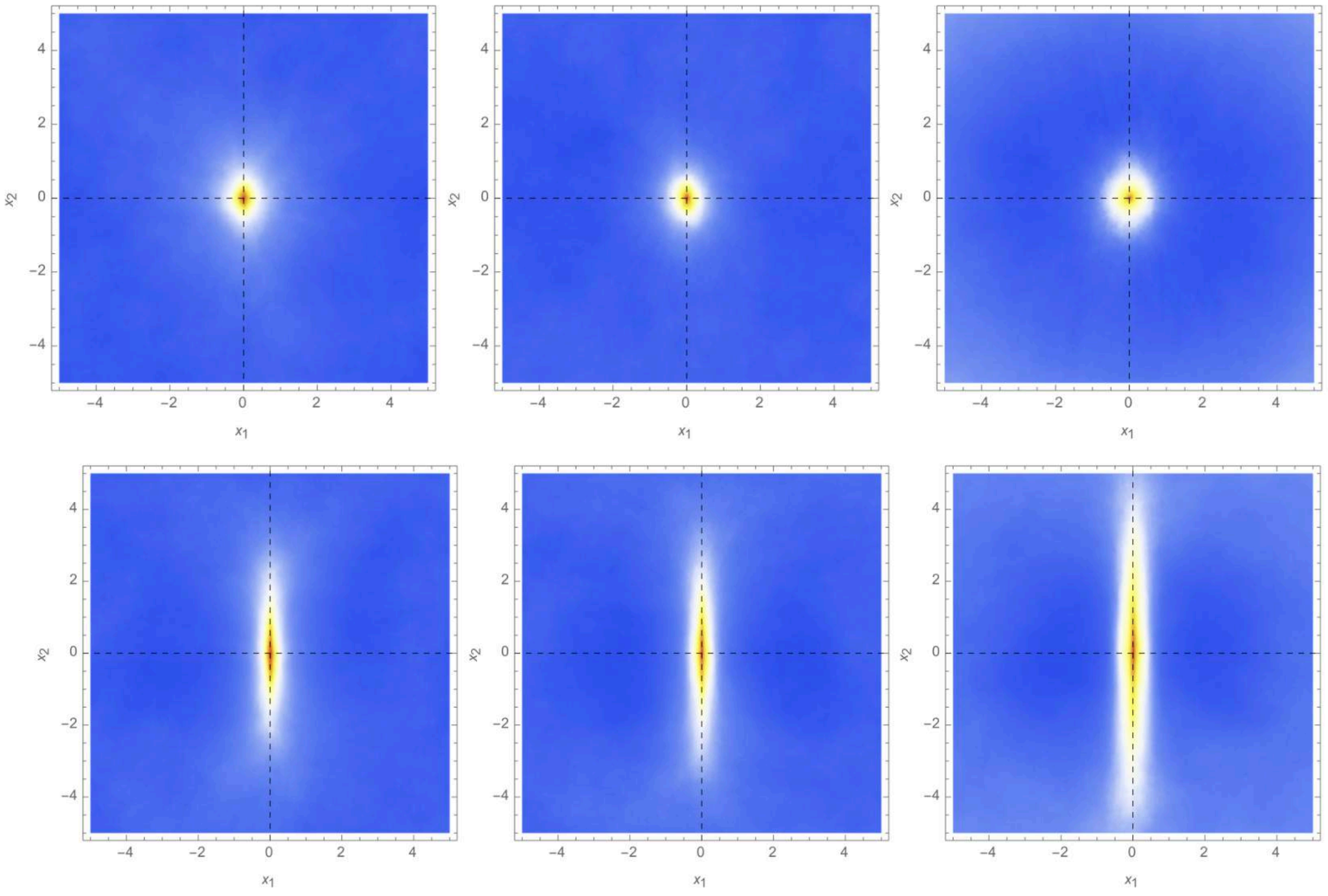

Cosmic web in 3D

Cusp Wall

$\lambda_1 = 1/b_+(t_c)$

$v_1 \cdot \nabla \lambda_1 = 0$

and

$0 > \lambda_2 > \lambda_3$

$v_2 \cdot \nabla(\lambda_2 + \lambda_3) = 0$

$v_3 \cdot \nabla(\lambda_2 + \lambda_3) = 0$

$\mathscr{H}(\lambda_2 + \lambda_3)$ **positive definite**

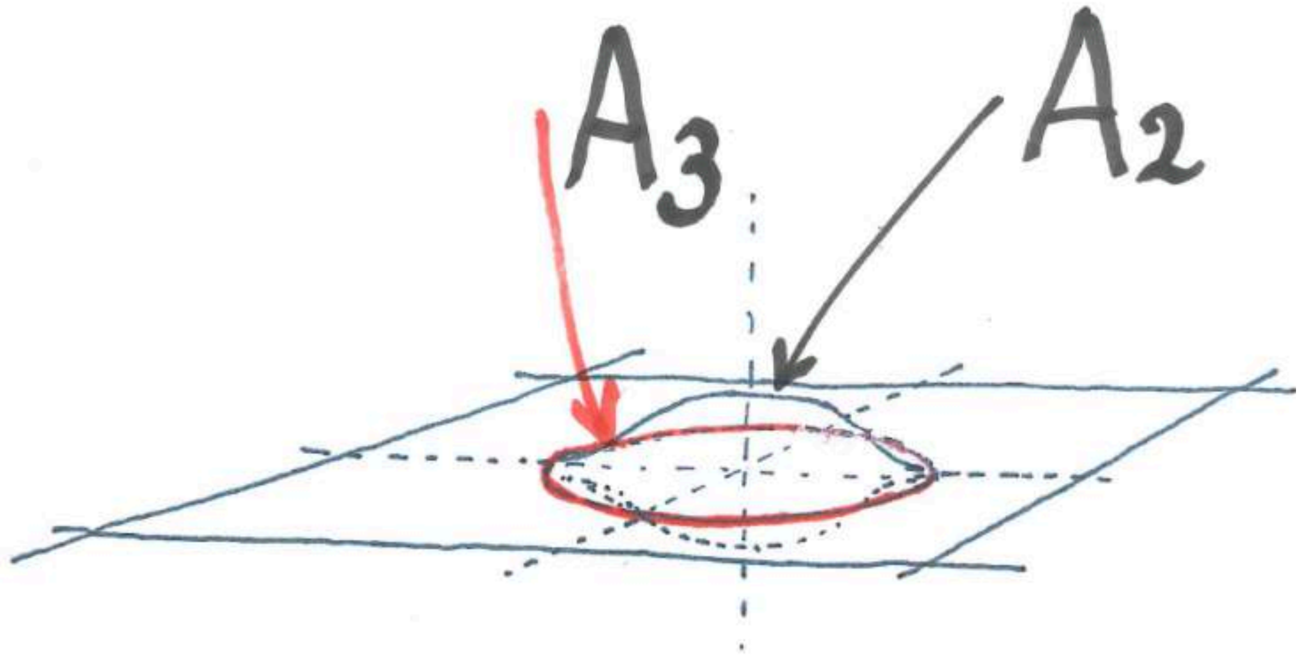

Swallowtail Filament

$\lambda_1 = 1/b_+(t_c)$

$v_1 \cdot \nabla \lambda_1 = 0$

$v_1 \cdot \nabla(v_1 \cdot \nabla \lambda_1) = 0$

and

$$\frac{\lambda_2(\boldsymbol{v}_3 \cdot \nabla(\boldsymbol{v}_1 \cdot \nabla\lambda_1))^2 + \lambda_3(\boldsymbol{v}_2 \cdot \nabla(\boldsymbol{v}_1 \cdot \nabla\lambda_1))^2}{(\boldsymbol{v}_2 \cdot \nabla(\boldsymbol{v}_1 \cdot \nabla\lambda_1))^2 + (\boldsymbol{v}_3 \cdot \nabla(\boldsymbol{v}_1 \cdot \nabla\lambda_1))^2} < 0$$

$$0 = ((\boldsymbol{v}_3 \cdot \boldsymbol{n}_c)\boldsymbol{v}_2 - (\boldsymbol{v}_2 \cdot \boldsymbol{n}_c)\boldsymbol{v}_3) \cdot \nabla \left[\lambda_2(\boldsymbol{v}_3 \cdot \boldsymbol{n}_c)^2 + \lambda_3(\boldsymbol{v}_2 \cdot \boldsymbol{n}_c)^2\right]$$

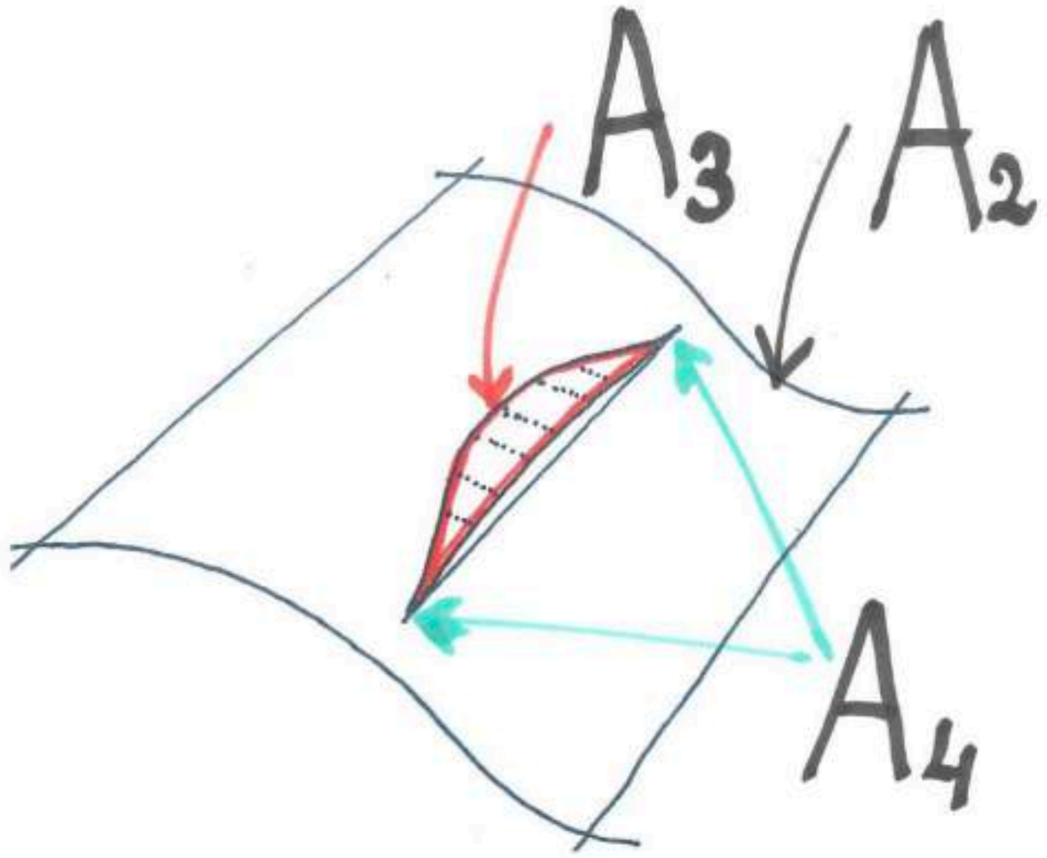

Umbilic Filament

$\lambda_1 = \lambda_2 = 1/b_+(t_c)$

and

$\lambda_3 < 0$

$v_3 \cdot \nabla \lambda_3 = 0$

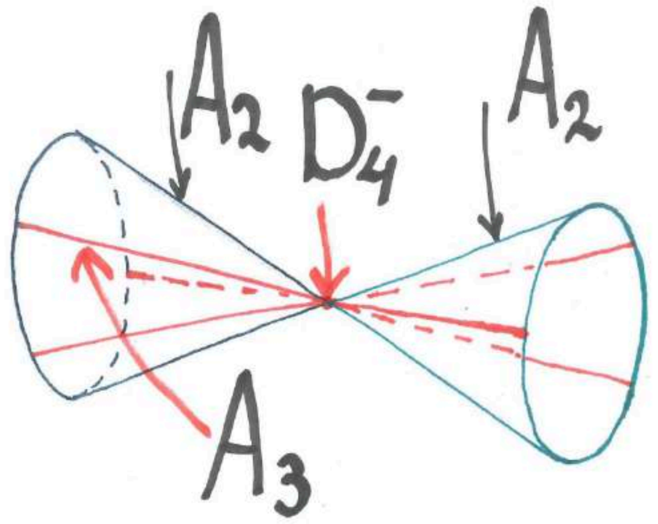

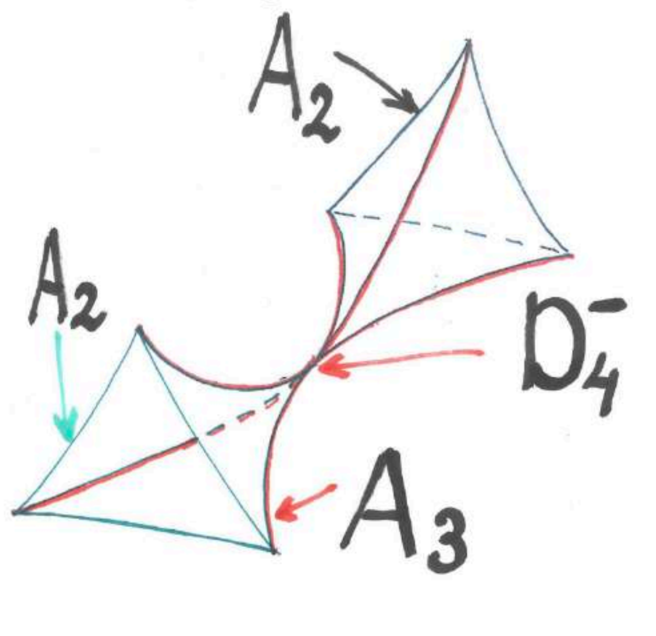

Cusp

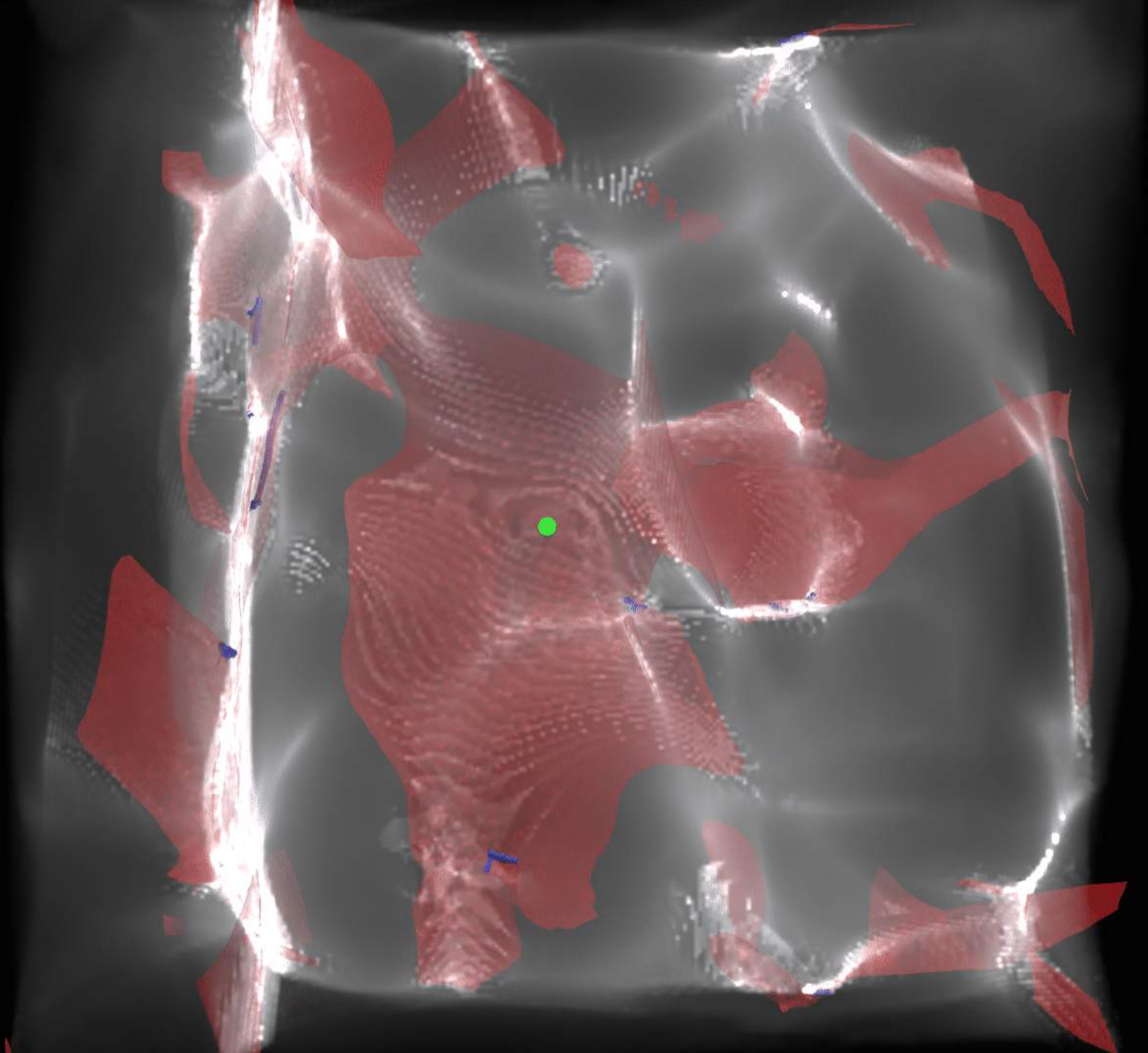

Swallowtail

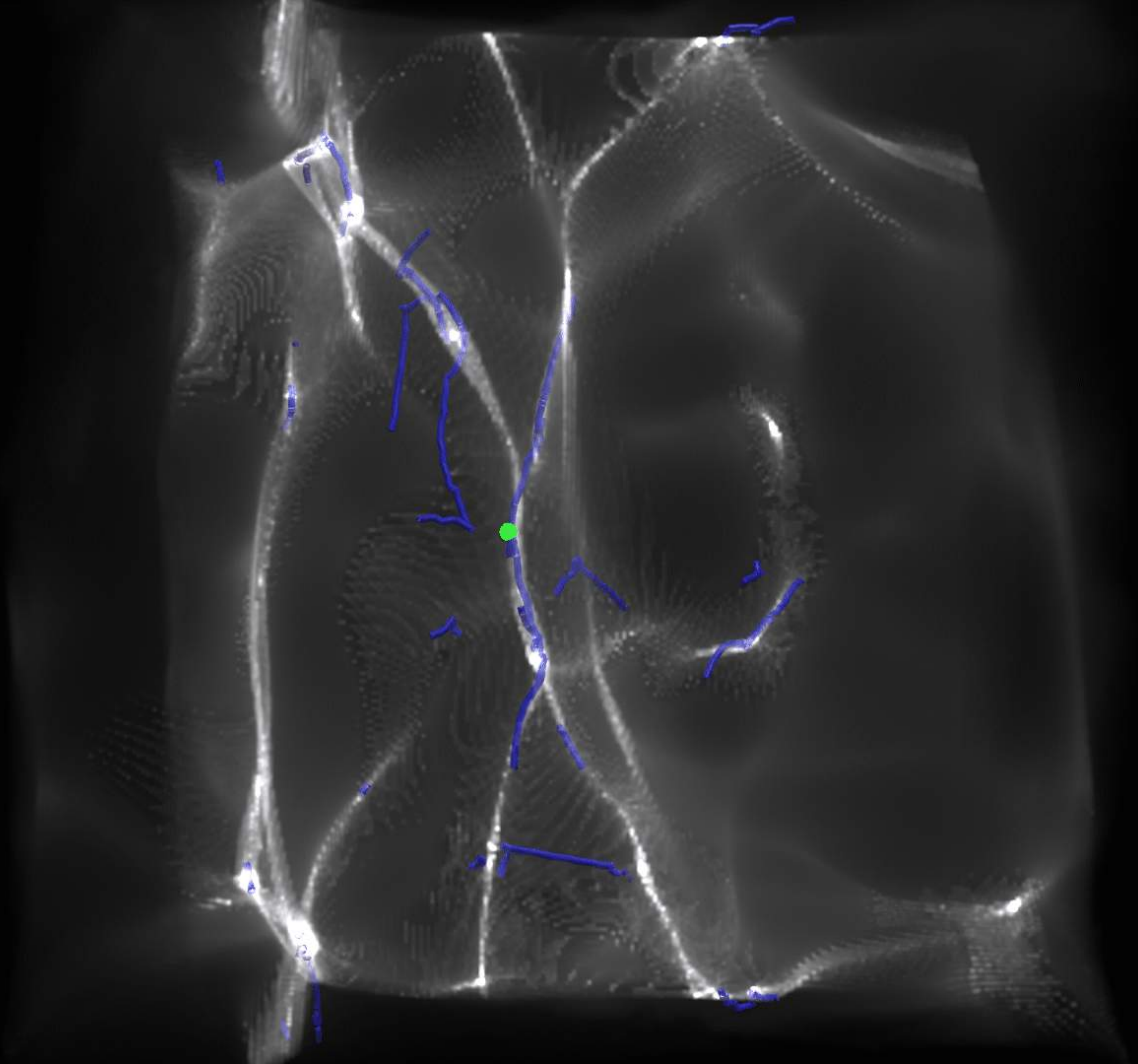

Umbilic

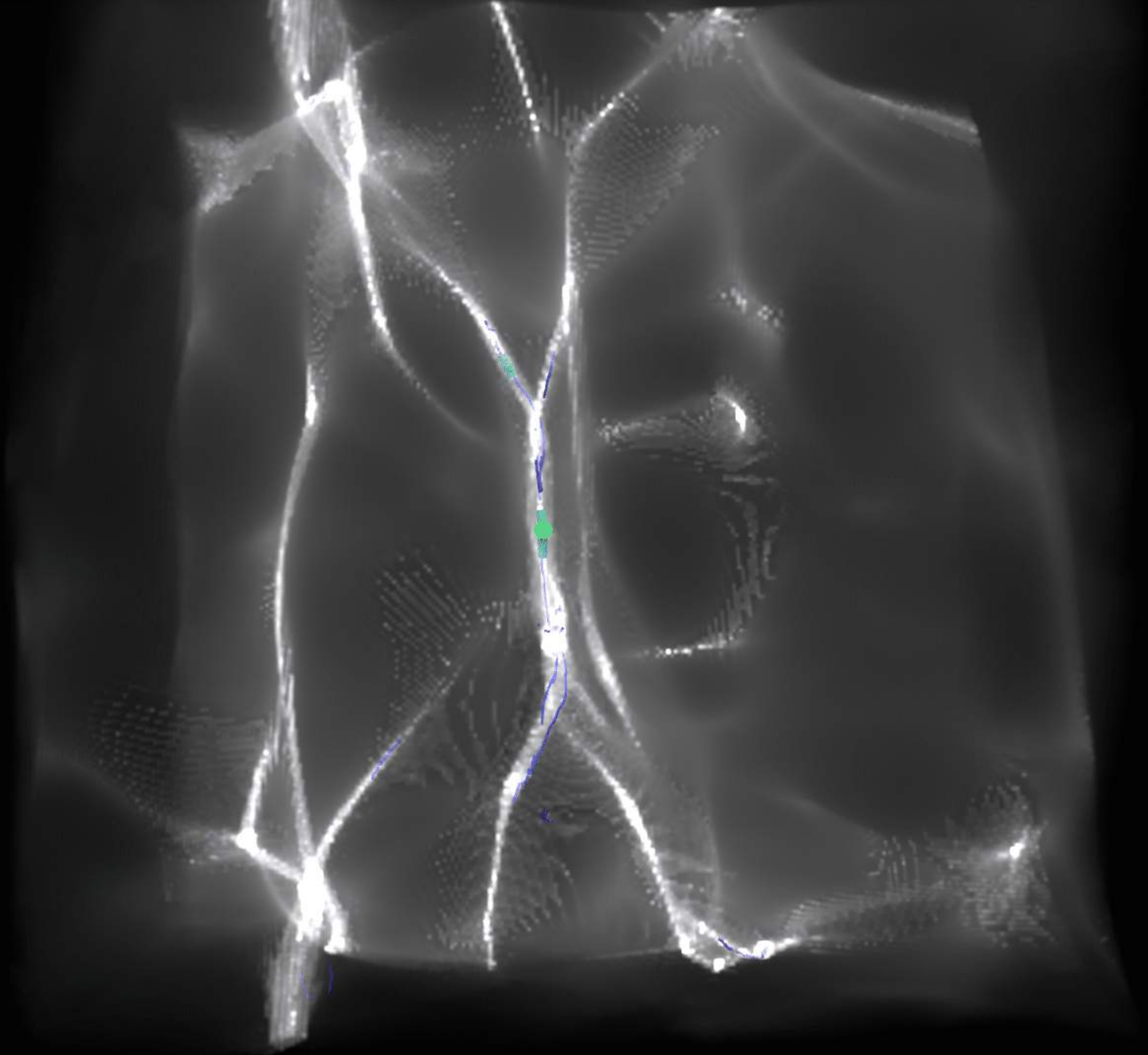

Constrained Gaussian Random field theory

By generating customized initial conditions, using non-linear constrained Gaussian random field theory, we can systematically study the different elements of the cosmic web

$$A_3^i(t) = \{\mathbf{q} \in L \mid \mathbf{q} \in A_2^i(t), \mathbf{v}_i \cdot \nabla \mu_{it} = 0\}$$

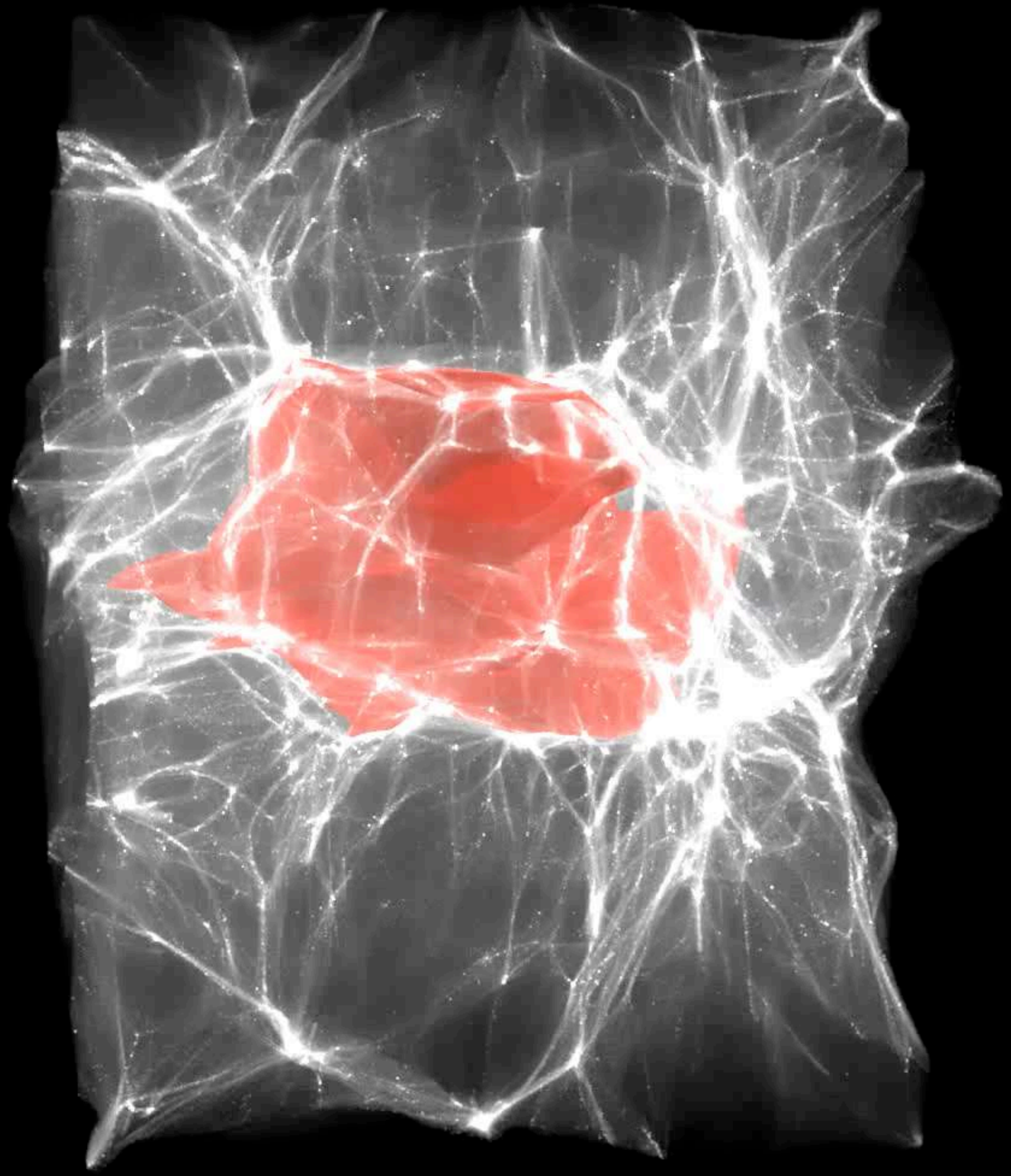

Constrained Gaussian Random field theory

By generating customized initial conditions, using non-linear constrained Gaussian random field theory, we can systematically study the different elements of the cosmic web

$$D_4^{ij}(t) = \{\mathbf{q} \in L \mid 1 + \mu_{it}(\mathbf{q}) = 1 + \mu_{jt}(\mathbf{q}) = 0\}$$

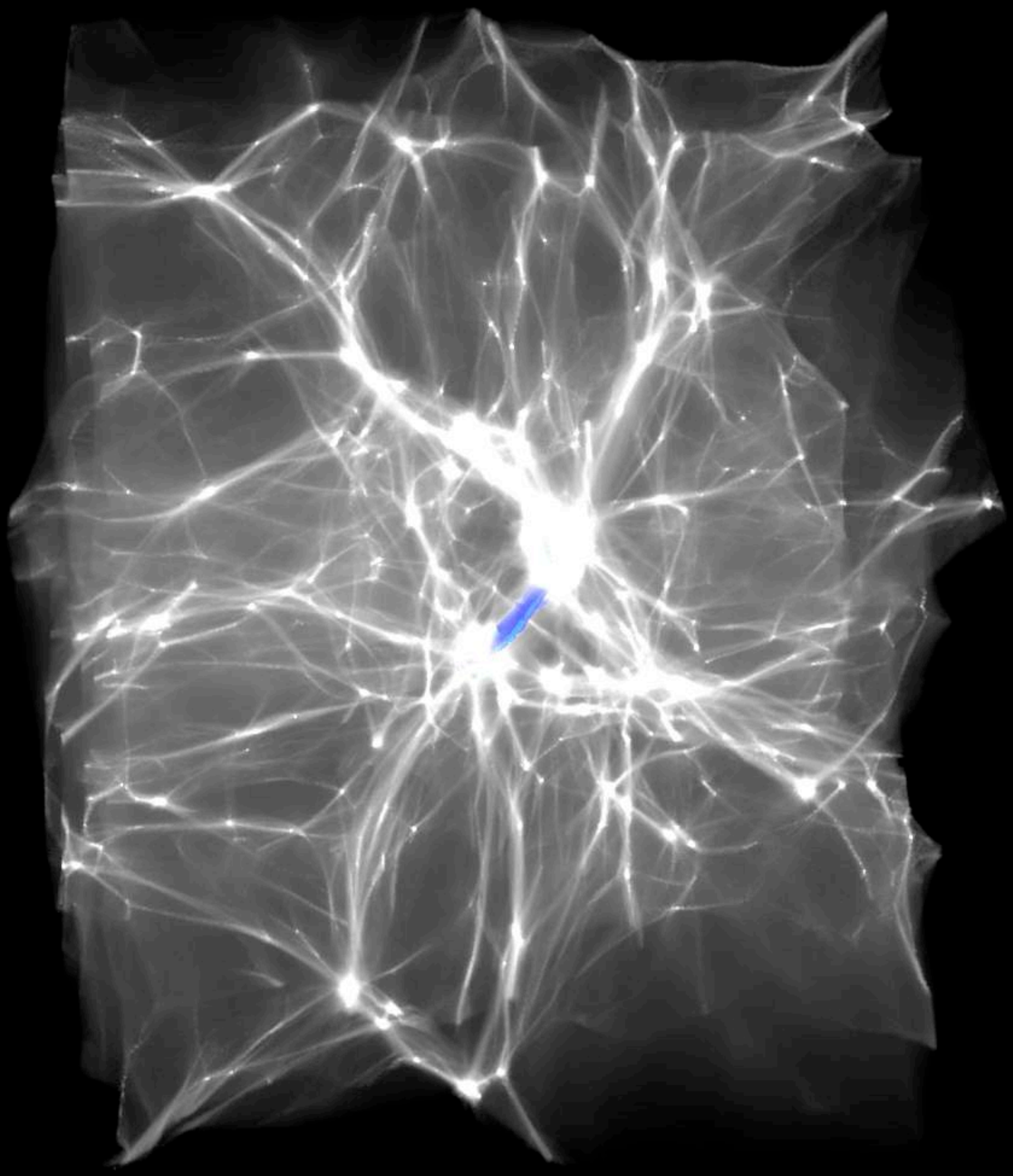

Conclusion

- The caustic skeleton of the cosmic web depends on the **eigenvalue** *and* **eigenvector fields**
- We construct a classification of the cosmic web based on the **formation history** rather than the **morphology** of the cosmic web
- We generate constrained **initial conditions** tied to the **dynamics of structure formation**
- **New condition** to identify **proto-walls** and **filaments**
- I am hopeful that this will **improve our understanding** of for example **galaxy alignments**